



1 **Comprehensive Automobile Research System (CARS) – a** 2 **Python-based Automobile Emissions Inventory Model**

3 Bok H. Baek¹, Rizzieri Pedruzzi², Minwoo Park³, Chi-Tsan Wang¹, Younha Kim³, Chul-Han
4 Song⁴, and Jung-Hun Woo³

5 ¹Center for Spatial Information Science and Systems – George Mason University, Fairfax, VA, USA.

6 ²Department of Sanitary and Environmental Engineering, Federal University of Minas Gerais, Belo Horizonte,
7 Brazil.

8 ³Department of Advanced Technology Fusion, Konkuk University, Republic of Korea

9 ⁴School of Earth and Environmental Engineering, Gwangju Institute Science and Technology, Republic of Korea

10 *corresponding to: Jung-Hun Woo (jwoo@konkuk.ac.kr)*

11

12 **Abstract**

13 The Comprehensive Automobile Research System (CARS) is an open-source python-based
14 automobile emissions inventory model designed to efficiently estimate high quality emissions
15 from motor-vehicle emission sources. It can estimate the criteria air pollutants, greenhouse gases,
16 and air toxics in various temporal resolutions at the national, state, county, and any spatial
17 resolution based on the spatiotemporal resolutions of input datasets. The CARS is designed to
18 utilize the local vehicle activity database, such as vehicle travel distance, road link-level network
19 Geographic Information System (GIS) information, and vehicle-specific average speed by road
20 type, to generate a temporally and spatially enhanced automobile emissions inventory for
21 policymakers, stakeholders, and the air quality modeling community. The CARS model adopted
22 the European Environment Agency's (EEA) onroad automobile emissions calculation
23 methodologies to estimate the hot exhaust, cold start, and evaporative emissions from onroad
24 automobile sources. It can optionally utilize road link-specific average speed distribution (ASD)
25 inputs to reflect more realistic vehicle speed variations by road type than a road-specific single
26 averaged speed approach. Also, utilizing high-resolution road GIS data allows the CARS to
27 estimate the road link-level emissions to improve the inventory's spatial resolution. When we
28 compared the official 2015 national mobile emissions from Korea's Clean Air Policy Support
29 System (CAPSS) against the ones estimated by the CARS, there is a moderate increase of VOC
30 (33%), CO (52%), and fine particulate matter (PM_{2.5}) (15%) emissions while NO_x and SO_x are
31 reduced by 24% and 17% in the CARS estimates. The main differences are driven by the usage of
32 different vehicle activities and the incorporation of road-specific ASD, which plays a critical role



33 in hot exhaust emission estimates but wasn't implemented in Korea's CAPSS mobile emissions
34 inventory. While 52% of vehicles use gasoline fuel and 35% use diesel, gasoline vehicles only
35 contribute 7.7% of total NO_x emissions while diesel vehicles contribute 85.3%. But for VOC
36 emissions, gasoline vehicles contribute 52.1% while diesel vehicles are limited to 23%. While
37 diesel buses are only 0.3% of vehicles, each vehicle has the largest contribution to NO_x emissions
38 (8.51% of NO_x total) due to its longest daily VKT. For VOC, CNG buses are the largest contributor
39 with 19.5% of total VOC emissions. It indicates that the CNG bus is better for the rural area while
40 the diesel bus is better applicable for the urban area for a better ozone control strategy because the
41 rural area is usually NO_x limited for ozone formation and urban area is VOC limited region. For
42 primary PM_{2.5}, more than 98.5% is from diesel vehicles. The CARS model's in-depth analysis
43 feature can assist government policymakers and stakeholders develop the best emission abatement
44 strategies.

45 Keywords: inventory: automobile, vehicle emissions, hot exhaust, cold start, evaporative, python

46 1 Introduction

47 Globally, ambient pollution causes more than 4.2 million premature deaths every year. Indoor
48 air pollution causes 3.8 million deaths and over 90% of people live in places where air pollutants
49 exceed the WHO standards (WHO, 2019; Hogrefe et al., 2001a; Hogrefe et al., 2001b; Dennis et
50 al., 2010; Rao et al., 2011; Appel et al., 2013; Luo et al., 2019). To effectively mitigate air
51 pollutants, both developed and developing countries' governments have been implementing
52 stringent air pollution abatement control policies to reduce harmful regional air pollutants.
53 Chemical transport models (CTM) are a powerful tool to study and develop an efficient control
54 strategy for local and regional air quality (Hogrefe et al., 2001a; Hogrefe et al., 2001b; Dennis et
55 al., 2010; Rao et al., 2011; Appel et al., 2013; Luo et al., 2019). The CTM simulation results
56 strongly rely on precise input data, such as emission inventory, meteorology, land surface
57 parameters, and chemical mechanisms in the atmosphere. The most dominant factor for accurate
58 CTM performance is temporally and spatially high-quality emissions, especially in the worst air
59 quality regions with significant anthropogenic emission sources.

60 The major anthropogenic emission sources in urban areas are from transportation emission
61 sectors. The tailpipe emissions from the vehicle's combustion process contain many air pollutants,
62 including nitrogen oxides (NO_x), volatile organic compounds (VOCs), carbon monoxide (CO),
63 ammonia (NH₃), sulfur dioxide (SO₂), and primary particulate matter (PM) which will participate
64 in the formation of detrimental secondary pollutants like ozone and PM_{2.5} in the atmosphere. In
65 the Seoul Metropolitan Area (SMA) in South Korea, transportation automobile sources contribute
66 the most to the total NO_x and primary PM_{2.5} emissions across all emission sources. While more
67 than 60% of total ambient PM_{2.5} are primary PM_{2.5} directly emitted from the sources, (Choi et al.,



68 2014; Kim et al., 2017a; Kim et al., 2017b; Kim et al., 2017c), the rest of the ambient PM_{2.5} are
69 secondary pollutant from heterogenous chemical reactions in the atmosphere during the
70 transportation. Thus, it is critical to understand and represent better on the emission patterns from
71 the transportation automobile sources in the CTM model. The use of process-based automobile
72 emission models is highly recommended to meet the needs in CTM model because it can estimate
73 the high quality spatiotemporal automobile emissions based on parameterizations of the emission
74 processes, such as physical, chemical, and vehicle operation processes from on/off-network roads
75 (Moussiopoulos et al., 2009; Russell and Dennis, 2000).

76 There are two methodologies known in emission inventory development: top-down and
77 bottom-up. The choice of methods is determined by the input data availability. The top-down
78 approach primarily relies on the aggregated and generalized country or regional information,
79 especially in developing countries where only limited datasets and information are available. It has
80 its limitations on representing the vehicle emission process realistically due to the lack of detailed
81 activity and ancillary supporting data. However, the bottom-up approach requires higher-quality
82 spatiotemporal activity datasets like road network information, vehicle composition (vehicle type,
83 engine size, vehicle age, and fuel-technology), pollutant-specific emissions factors, road segment
84 length, traffic activity data, and fuel consumption (EEA, 2019; Ibarra-Espinosa et al., 2018b;
85 IEMA, 2017). It can generate more accurate and detailed automobile emissions across various
86 operating processes, such as hot exhaust, evaporative, idling, and hot soak (Nagpure et al., 2016;
87 Ibarra-Espinosa et al., 2018a).

88 There are several bottom-up mobile emissions models available, like MOVES (MOtor
89 Vehicle Emissions Simulator) from the U.S. Environmental Protection Agency (USEPA), the
90 European Environment Agency's (EEA) model COPERT (COmputer Programmed to calculate
91 Emissions from Road Transport), the HERMES (High-Elective Resolution Modelling Emission
92 System) from Barcelona Supercomputing Center (Guevara et al., 2019), the VEIN (Vehicular
93 Emissions INventory) model developed by Ibarra-Espinosa et al. (2017), and the VAPI (Vehicular
94 Air Pollution Inventory) model developed by Nagpure and Gurjar (2012) for India (Nagpure et al.,
95 2016). While these models are all bottom-up emission inventory models, a single model cannot
96 meet all modelers, policymakers, and stakeholders' needs because each model holds its own pros
97 and cons. They are developed differently to meet their own needs based on the types of traffic
98 activity and emission factors, emission calculation methodologies, and other optional/available
99 traffic-related inputs such as average speed distribution and geographical resolution. The bottom-
100 up emission calculations can be further complicated when other factors like emissions factors with
101 varying vehicle operation speeds and local meteorology are accounted for.

102 The MOVES model has the strength to generate high-quality emissions for up to 16
103 different emission processes (i.e., Running Exhaust, Start Exhaust, Evaporative, Refueling,
104 Extended Idling, Brake, Tire, etc.). It can simulate not only county-level but also road segment
105 level depending on data availability. It can also reflect local meteorological conditions, such as



106 ambient temperature and relative humidity, which can significantly impact both pollutants and
107 emissions processes (Choi et al., 2017; Perugu et al., 2018). Disadvantages of this model are the
108 lack of transparency for emission factors and algorithms and that it is computationally expensive
109 to generate these high-quality emissions inventories (Li et al., 2016; Xu et al., 2016; Liu et al.,
110 2019; Perugu, 2019). The COPERT model that is widely used in European countries has its
111 advantages, such as the capability to model emissions in high resolution. Additionally, it is fully
112 integrated with the EEA's onroad vehicle emissions factors guidelines and can generate a complete
113 quality assurance (QA) and visualization summary (Ntziachristos et al., 2009). The cons are that
114 it is a proprietary commercial licensed software, limited to EEA guidance, and challenging to
115 modify and update with any key input datasets like the latest emission factors from non-European
116 countries (Lejri et al., 2018; Rey DR, 2018; Li et al., 2019; Lv et al., 2019; Smit et al., 2019).

117 The HERMES and VEIN are both recently released bottom-up inventory models. They
118 have their pros in that they are both open-source models based on open-source computing
119 languages (Python and R), which provide transparency of emission calculations with a
120 considerable amount of data behind it (Ibarra-Espinosa et al., 2018b; Guevara et al., 2019). Both
121 models are driven by comma-separated value (CSV) formatted input files, making it very easy for
122 users to modify the input datasets. They are also based on the EEA's emission calculation method
123 and equipped with a complete QA and visualization tool based on Python and R libraries. However,
124 it is not an easy task to update the emission factors, and generate other required input datasets for
125 other countries, and lacks support for any control strategy plan feature to generate a responsive
126 reduced emissions inventory for policymakers, stakeholders, and modelers.

127 The VAPI (Vehicular Air Pollution Inventory) model was developed in India because the
128 country does not have an extensive and robust traffic-related dataset to run these kinds of vehicular
129 emissions inventory models (Nagpure et al., 2016; Perugu, 2019).

130 There are also a few shortcomings of incorporating these bottom-up models into CTM
131 studies. These models require strong programming skills to operate, such as collecting and
132 preparing the input data to fit the model requirement, configuring the model variables, and
133 changing specific variables that may be hidden somewhere. Another downside is that while the
134 administration-level emissions inventory can be estimated by those models, it requires a 3rd party
135 emissions processor like the SMOKE (Sparse Matrix Operator Kernel Emissions) modeling
136 system (Baek and Seppanen, 2021) to process and generate spatially and temporally resolved
137 emissions inputs for CTM. Some detailed information, like link-level hourly driving patterns, can
138 be lost in the emissions processing steps.

139 There is no single model capable of meeting all the requirements across various spatial and
140 temporal scales (Pinto et al., 2020). However, transparency, simplicity, and a user-friendly
141 interface are requirements for those who mainly work in transportation policy and air quality
142 modeling development (Fallahshorshani et al., 2012; Kaewunruen et al., 2016; Sallis et al., 2016;



143 Sun et al., 2016; Tominaga and Stathopoulos, 2016). Thus, the ideal mobile emissions modeling
144 system would be computationally optimized, easy-to-use, and have a user-friendly interface.
145 Additionally, the model should easily adapt detailed local activity information and the state-of-art
146 emission factors as an input to represent them in the highest resolution possible in time and space.

147 We have developed the Comprehensive Automobile Research System (CARS) to meet these
148 requirements, especially for the air quality research community, policymakers, and air quality
149 modelers. The CARS is a stand-alone, fully modularized, computationally optimized, python-
150 based automobile emission model. The modularization improves the efficiency of processing times.
151 Once district and road-link level annual/monthly/daily total emissions are computed, the rest of
152 the processes are optional. It can generate chemically speciated, spatially gridded hourly emissions
153 for CTMs without any 3rd party emissions modeling system to develop the highest quality CTM-
154 ready emissions inputs. All functions are operated by independent modules and can be enabled by
155 users. Details on modularization will be discussed later. The CARS model can be easily adopted
156 and is simple for users to add new functions or modules in the future. The application of the CARS
157 to South Korea will be described in detail later.

158 **2 CARS Emissions Calculation**

159 The CARS is an open-source Python-based customizable motor vehicle emissions
160 processor that estimates onroad and offroad emissions for specific criteria and toxic air pollutants.
161 Figure 1 is a schematic of the CARS overview. It applies vehicle, engine, and fuel specific
162 emission factors to traffic data to estimate the local level annual, monthly, and daily total emissions
163 inventory. The emissions inventory calculations require the list of pollutant-specific emissions
164 factors by vehicle age, local activity data, average speed profile/distribution by road type, and
165 geographic information system (GIS) road segment shapefiles inputs. The spatial resolution of
166 VKT defines the CARS geographic scale (i.e. district, county, state, and country) for emission
167 calculations. Unlike the district-level Korea Clean Air Policy Support System (CAPSS)
168 automobile emission inventory (Lee et al., 2011a; Lee et al., 2011b), the CARS applies high-
169 resolution annual average daily traffic (AADT) data from the road GIS shapefiles to distribute the
170 total district emissions into road link-level emissions. Optionally, these road link-level emissions
171 can be used to generate spatially gridded CTM-ready emissions input data once the output
172 modeling domain is defined. How the CARS estimates spatially and temporally enhanced
173 automobile emissions inventories will be discussed in detail next chapter.

174 South Korean traffic databases by the Korea CAPSS team (Lee et al., 2011b) from the
175 National Institute of Environmental Research (NIER) were used in this study to compute the
176 updated onroad automobile emissions inventory. The databases include individual vehicle activity
177 data (daily total VKT), road activity data (average speed distribution by road), vehicle age specific
178 emission factors, road type information, surface weather data, and GIS road shapefiles.



179 2.1 Individual Daily Total VKT Activity Data

180 The accuracy of vehicle emissions inventories from CARS significantly depends on the
181 quality of traffic density information. To accurately represent traffic density for the CARS, this
182 study imported the national registered vehicle-specific daily total VKT from South Korea's
183 Vehicle Inspection Management System (VIMS), which belongs to the Korea Transportation
184 Safety Authority (KTSA). It contains over 50 million records from 2013 to 2017. For the CARS
185 model, we first sorted these records by the vehicle identification number (VIN) to remove any
186 duplicates and then built vehicle-specific daily total VKT traffic activity data in the CSV format.
187 The summary of those vehicle numbers and VKTs is presented in Fig. 2. Sedan vehicles using
188 gasoline fuel comprise the greatest percentage of total vehicles at 47% (~10.4 million) and have
189 the highest VKT. Most vehicles demonstrate similar patterns between the number of vehicles and
190 daily VKT. However, as expected, LPG (liquefied petroleum gas)-fueled taxi are high in VKT
191 compared to the number of vehicles due to their daily long distance travel pattern.

192 Besides the numbers of vehicles, the vehicle type (v) and the VIN are applied to individual
193 vehicles to calculate their daily total VKT or $VKT_{v,age}$ (km d^{-1}). In Eq. (1), the individual vehicle
194 VKT with the manufactured year ($VKT_{v,age}$) is calculated based on the cumulative mileage (M_f)
195 since the last inspection date (D_f) and registration date (D_0). Korea's NIER defines the vehicle
196 types (Ryu et al., 2003; Ryu et al., 2004; Ryu et al., 2005; Lee et al., 2011a) based on a combination
197 of vehicle types (e.g., sedan, truck, bus, etc), engine sizes (e.g., compact, full size, midsize, etc)
198 and fuel types (e.g., gasoline, diesel, LPG, etc). Full details of vehicle types and daily total VKT
199 are shown in Appendix A and B.

$$200 \quad VKT_{v,age} = \frac{M_{f,v,age}}{D_{f,v,age} - D_{0,v,age}} \quad (1)$$

201 2.2 Emission Calculations

202 Automobile emission sources cover motorized engine sources from network (onroad) and
203 off-network (nonroad). Nonroad transportation sources represent any motorized engine vehicle
204 emissions that occurred from off-network roads, such as aviation, railways, construction, and boats.
205 Onroad automobile emissions are ones that occur on the network roads. While nonroad automobile
206 emissions are important, we will focus on the onroad automobile emissions from network roads
207 using their local traffic-related datasets. The following section explains the approach of the onroad
208 automobile emission processes. The onroad emission (E_{onroad}) in the CARS is defined in Eq. (2),
209 which includes three major emission processes (Ntziachristos and Samaras, 2000):

$$210 \quad E_{onroad} = E_{hot} + E_{cold} + E_{vap} \quad (2)$$



211 The hot exhaust emissions (E_{hot}) are the vehicle's tailpipe emissions when the internal combustion
212 engine (ICE) combusts the fuel to generate energy under the average operating temperature. The
213 cold start emissions (E_{cold}) are the tailpipe emissions from the ICE when the cold vehicle engine is
214 ignited and the operational temperature is below average condition. The evaporative VOC
215 emissions (E_{vap}) are the emissions evaporated/permeated from the fuel systems (fuel tanks,
216 injection systems, and fuel lines) of vehicles.

217 The CARS first applies the hot exhaust emission factors by vehicle type, age, fuel, engine,
218 and pollutants to individual daily total VKT to compute the hot exhaust emissions. The rest of the
219 processes for cold start and evaporative emissions are calculated afterwards. The emission
220 calculation methodologies used in the CARS model are based on tier 2 and tier 3 methodologies
221 from the EEA's mobile emission inventory guidebook (EEA, 2019) to be consistent with Korea's
222 National Emission Inventory System (NEIS) (Lee et al., 2011a).

223 2.2.1 Hot Exhaust Emissions

224 Hot exhaust emission, which is from the vehicle's tailpipe, is the exhaust gas from the
225 combustion process in an ICE. The ICE combustion cycle generally causes incomplete combustion
226 processes which emit hydrocarbons, carbon monoxide (CO), and particulate matter (PM) into the
227 atmosphere. The sulfur compounds in the fuel are oxidized and become sulfur oxides (SO_x).
228 Nitrogen oxides (NO_x) are similarly produced during the combustion process due to the abundant
229 nitrogen (N₂) and oxygen (O₂) in the atmosphere.

230 Equation 3 represents the calculation of daily individual vehicle hot exhaust emission rate,
231 $E_{hot;p,v,age}$ (g d⁻¹) of pollutant (p). An individual vehicle-specific daily $VKT_{v,age}$ (km d⁻¹) is estimated
232 by Eq. (1). The $EF_{hot;p,v,age,s}$ (g/km) is the hot exhaust emission factor of pollutants (p) for the
233 vehicle type (v), vehicle age (age), and average vehicle speed (s). The district's total emission rate
234 is the total hot exhaust emissions from all individual vehicles within the same district.

$$235 \quad E_{hot;p,v,age} = DF_{p,v,age} \times VKT_{v,age} \times EF_{hot;p,v,age,s} \quad (3)$$

236 The deterioration factor (DF) in Eq. (3) is an optional function in the CARS model that can
237 be turned on or off by users. This deterioration process is caused by vehicle aging and can lead to
238 the increase of vehicle emissions. The CARS model applies the vehicle registration year to
239 estimate the deterioration factor as additional emissions, which vary by vehicle type and pollutant.
240 According to the guidance of deterioration factors calculation from NIER, there is no deterioration
241 in a new vehicle in their first five years. After five years, the deterioration factors can increase the
242 range by 10% depending on the type of vehicle and pollutants. Deterioration processes can cause
243 a 50% or 100% increase of emissions in fifteen-year-old vehicles. Currently, the DF is an empirical
244 coefficient that varies by vehicle age (Lee et al., 2011a).



245 The hot exhaust emission factor, $EF_{hot;p,v,s}$ (g/km) is a function of vehicle speed (s) with
246 other empirical coefficients: a, b, c, d, f, k . The emission factor formula and those coefficients were
247 developed by NIER CAPSS (Lee et al., 2011a). These coefficients are varied by pollutants (p),
248 vehicle type (v), vehicle age (age), and vehicle speed (s). The vehicle speed affects the combustion
249 efficiency of an ICE and impacts the emission rates and its composition from the tailpipe.

$$250 \quad EF_{hot;p,v,age,s} = k(a \times s^b + c \times s^d + f) \quad (4)$$

251 While vehicle speed plays a critical role in hot exhaust emissions from most vehicles, NO_x
252 emissions from some diesel vehicles show sensitivity to local ambient temperature along with
253 vehicle speed (Ntziachristos and Samaras, 2000). Figure 3 shows the dependency of NO_x emission
254 factors from compact diesel vehicles to vehicle speed (Fig. 3a) and ambient temperature (Fig. 3b).
255 Figure 3a shows a significant decrease of NO_x emissions while speed increases. Figure 3b
256 demonstrates the significance of local meteorology on NO_x emissions from a compact diesel sedan.
257 Based on these NIER's CAPSS emission factors, the sensitivity to local ambient temperature is
258 limited to NO_x pollutant emissions from diesel vehicles.

259 Due to its high sensitivity to the vehicle operating speed, it is important for the CARS to
260 simulate realistic speed patterns for accurate emissions estimates. When a constant single speed is
261 assigned to compute hot exhaust emissions, it won't reflect the emissions under low-speed
262 circumstances, which could cause higher emissions due to its incomplete ICE combustion. To
263 overcome this limitation, the CARS has adopted the 16 average speed bins concepts for a better
264 representation of vehicle speed distribution that varies by road type (i.e., local, highway,
265 expressway). We have implemented a feature for the CARS optionally to apply road-specific
266 average speed distributions (ASD) ($A_{bin,r}$), which represents the fractions of 16-speed bins (bin)
267 (from 0 to 121 km h⁻¹ defined in Appendix E) for eight different road types (r) (No.101-108, shown
268 in Appendix C) as classified by CAPSS (Fig. 4). Although ASD patterns vary by region, we did
269 not implement the regional variations of ASD due to the lack of region-specific vehicle speed
270 measurements in South Korea.

271 In this study, we developed the most realistic ASDs for eight different road types (No. 101-
272 108) in South Korea based on the latest road link-specific average speed and AADT from the GIS
273 road network shapefiles (NIER, 2018) and the U.S. EPA's MOVES ASD datasets (USEPA, 2020).
274 Because a single average speed was assigned to each road link, the ASDs based on South Korea's
275 GSI road shapefiles did not capture the low-speed range (<16 km h⁻¹) that occurs in reality.
276 Therefore, we incorporated the ASD developed by U.S. EPA with Georgia state ASD to improve
277 the representation of the low-speed range (speed bin #1 and #2). We modified the total fractions
278 of low-speed bins (the 2:1 ratio of fractions of bin #1 and #2) by adding 2% of distribution for
279 interstate expressways, 3% of distribution for urban expressways, 7% of distribution for all
280 highways, and 15% for all local roads. Further, those increases of low-speed bins reduced the



281 distributions of other higher speed bins homogeneously due to the renormalization of fractions by
282 road type. Figure 4 shows the renormalized ASDs of all road types applied in this study.

283 While 16-speed bins ASD application is critical to computing more realistic hot exhaust
284 emissions, there should be some restrictions on certain road types. Users can adjust the restricted
285 roads control table input file to limit the vehicle types that can only be operated on a particular
286 road type. For example, motorcycles are limited to local roads (No. 104, 106, and 107), but not on
287 expressways (No. 101, 102, 103, 105, and 108) due to its traffic regulation rules. Heavy trucks are
288 only allowed on the highway (No. 101, 102, 103, 105, and 108.) by law. The details of the road
289 restriction control table format can be found on the CARS's user's guide from the CARS Github
290 website (https://github.com/bokhaeng/CARS/tree/master/docs/User_Manual).

291 The 16-speed bins averaged speed distribution calculated by road type ($A_{bin,r}$) and road type
292 weight factors ($\omega_{r,d}$) in a district (d) from Eq. (13) are added to the CARS hot exhaust emissions
293 equation (Eq. 3). The hot exhaust emissions from individual vehicles ($E_{hot;p,v,age}$) can be calculated
294 by considering road-specific speed bins distribution (Eq. 5). Although the vehicles may be
295 operated in different districts from their registered district, this is our best method to estimate the
296 vehicle speed for hot exhaust emissions.

$$297 \quad E_{hot;p,v,age} = DF_{p,v,age} \times \sum_{bin} (VKT_{v,age} \times EF_{hot;p,v,age,s} \times A_{bin,r}) \quad (5)$$

298 2.2.2 Cold Start Emissions

299 The cold start emissions occur when a cold-engine vehicle is ignited. The lower
300 temperature of the ICE is not an optimal condition for complete fuel combustion. This process
301 lowers the combustion efficiency (CE) and increases the emissions of hydrocarbon and CO
302 pollutants from the tailpipe exhaust (Jang et al., 2007). The CARS can estimate the cold start
303 emissions for vehicles using gasoline, diesel, or liquefied petroleum gas (LPG) fuel. Besides the
304 vehicle and engine type, road type also plays a critical role in the quantity of cold start emissions
305 because it occurs mostly in parking lots and rarely on highways.

306 The cold start emission, E_{cold} (g d^{-1}), is derived from the hot exhaust emissions, the ratio of
307 hot to cold exhaust emissions ($EF_{cold}/EF_{hot} - 1.0$), and the percentage of the traveled distance with
308 a cold engine (Eq. 6).

$$309 \quad E_{cold;p,v} = \beta_T \times E_{hot;p,v} \times \left(\frac{EF_{cold;p,v}}{EF_{hot;p,v}} - 1.0 \right) \quad (6)$$

310 The emission factor of cold start emissions (EF_{cold}) is not directly calculated from
311 measurement data like hot exhaust emissions ($E_{hot;p,v}$), but measured under different ambient
312 temperatures (T). The CARS model applies linear regression models developed by CAPSS to
313 estimate the increasing ratio of cold start to hot exhaust emissions (EF_{cold}/EF_{hot}) under different



314 temperatures (T) (Eq. 7). In this equation, A and B are the empirical coefficients that vary by the
315 pollutants (p) and vehicle type (v).

$$316 \quad \left(\frac{EF_{cold; p,v}}{EF_{hot; p,v}} \right) = A_{p,v} + B_{p,v} \times T \quad (7)$$

317 β is the percentage of the distance traveled under a cold engine. It also depends on the
318 ambient temperature. Cold ambient temperatures cause a longer distance traveled under a cold
319 engine due to the slower heating time. According to the CAPSS database for Seoul city (Lee et al.,
320 2011a), the empirical linear equation for β is shown in Eq. (8). This formula represents how
321 ambient temperature affects β . For example, when the average temperature is -2°C , β is 34.8%.
322 In summer, the monthly average temperature is 25.7°C , which causes β to drop to 21%.

$$323 \quad \beta = 0.647 - 0.025 \times 12.35 - (0.00974 - 0.000385 \times 12.35) \times T \quad (8)$$

324 2.2.3 Evaporative VOC Emissions

325 Evaporative emissions are emissions from vehicle fuel that are evaporated into the
326 atmosphere. This occurs in the fueling system inside the vehicle, such as fuel-tanks, injection
327 systems, and fuel lines. Diesel vehicles, however, can be exempted due to diesel fuel's low vapor
328 pressure. The primary sources of evaporative emissions are breathing losses through tank vents
329 and fuel permeation/leakage. The CARS model adopted the EEA's emission inventory guidebook
330 (EEA, 2019) to account for three mechanisms to estimate the evaporative VOC emissions (E_{vap}):
331 diurnal emissions from the tank (e_d), hot and warm soak emissions by fuel injection type (S_{fi}), and
332 running loss emissions (R) (Eq. 9). Unlike CAPSS, there is a conversion factor (0.075) applied to
333 E_{vap} for motorcycles to prevent an over-estimation of VOC.

$$334 \quad E_{vap; p,v} = (e_{d; p,v} + S_{fi; p,v} + R_{l; p,v}) \quad (9)$$

335 Diurnal emissions, e_d (g d^{-1}), during the daytime are caused by the ambient temperature
336 increase and the expansion of fuel vapors inside the fuel tank. Most of the current fuel tank systems
337 have emission control systems to limit this kind of evaporative VOC emissions. The e_d can be
338 calculated with the empirical Eq. (10), which was developed by CAPSS. T_l is the monthly average
339 of the daily lowest temperatures and T_h is the monthly average of the daily highest temperatures.
340 The empirical coefficient α is 0.2, which represents how 80% of emissions are eliminated by the
341 vehicle emission control system.

$$342 \quad e_d = \alpha \times 9.1 \exp[0.3286 + 0.0574 \times (T_l) + 0.0614 \times (T_h - T_l - 11.7)] \quad (10)$$

343 Soak emissions (S_{fi}) occur when a hot ICE is turned off; the remaining heat from the ICE
344 can increase the fuel temperature in the system. The carburetor float bowls are the major source of



345 the soak emissions. Newer vehicles with fuel injection and return-less fuel systems do not emit
346 soak emissions. Because most of the current vehicles in South Korea have a new fuel system, soak
347 emissions (S_{fi}) in the CARS model are set to 0.

348 The running loss emissions (R_l) are from vapors generated in the fuel tank when a vehicle
349 is in operation (Eq. 11). In some older vehicles, the carburetor and engine operation can increase
350 the temperature in the fuel tank and carburetor, which can cause a significant increase in
351 evaporative VOC emissions. VOC emissions from running loss can be greatly increased during
352 warmer weather. However, newer vehicles with fuel injection and return-less fuel systems are not
353 affected by the ambient temperature. Because most vehicles in South Korea do not use carburetor
354 technology, we expect running loss emissions to have the least impact (Lee et al., 2011b).

$$355 \quad R_l = \alpha \times L_{r,v} \times [(1 - \beta) \times R_h + \beta \times R_w] \quad (11)$$

356 The empirical coefficient α is 0.1 here, which represents that 90% of the running loss is
357 avoided by the newer fuel system. L is the distance traveled (km) by road and is the same one used
358 in hot exhaust emission calculations. β is the same parameter from Eq. (8). The R_h and R_w are the
359 average emission factors from running loss under hot and warm/cold conditions, respectively.

360 **2.3 Road Link-Level Emissions Calculations**

361 In general, district-level automobile emissions calculations are driven by district-level
362 averaged vehicle activity and operating data, which do not reflect realistic spatial patterns of
363 onroad automobile emissions. The CARS model introduces road link-specific traffic data by
364 default to develop spatially enhanced road link-specific emissions that reflect more representative
365 emissions by road link. This high-resolution traffic data is a GIS shapefile that is composed of
366 many connected segments, which are called “road links.” All road links hold information such as
367 start/end location coordinates, AADT, road link length, averaged vehicle speed, and road type (No.
368 101-108).

369 The CARS model applies link-level AADT ($AADT_{d,r,l}$, d^{-1}) and road length ($L_{d,r,l}$) to
370 compute the road link-specific VKT ($VKT_{d,r,l}$, $km\ d^{-1}$) in Eq. (12). The road links are identified by
371 district (d), road type (r), and link (l) labels. The road VKT is a parameter that reflects the traffic
372 activity of each road link and it is different from individual daily vehicle activity data ($VKT_{v,age}$)
373 in Eq. (1).

$$374 \quad VKT_{d,r,l} = AADT_{d,r,l} \times L_{d,r,l} \quad (12)$$

375 Road link-specific VKT ($VKT_{d,r,l}$) is used to redistribute the district total emissions (E_{onroad})
376 from Eq. 2 into road link-level emissions. The following three weight factors are computed: the
377 district weight factors, ω_d (Eq. 13), the road type weight factors, $\omega_{d,r}$ (Eq. 14), and the road-link



378 weight factors, $\omega_{d,l}$ (Eq. 15). The weight district factors (ω_d) are the renormalization of each
379 district's total VKT over state-level total VKT (N is the number of districts). The main reason we
380 performed the renormalization over state-level total VKT is to reflect daily traffic patterns from
381 multiple districts under the assumption that most vehicles travel within the same state. The road
382 type weight factors by district ($\omega_{r,d}$) are used to compute road-specific emissions, while road-
383 specific averaged speed distributions (ASD; $A_{s,r}$) from Eq. (5) are applied to capture vehicle
384 operating speeds by road type. The road link weight factors ($\omega_{d,l}$) are then applied to redistribute
385 the district emissions into road link-level emissions.

386

$$387 \quad \omega_d = \frac{\sum_r \sum_l VKT_{d,r,l}}{\frac{1}{N} \sum_d \sum_r \sum_l VKT_{d,r,l}} \quad (13)$$

$$388 \quad \omega_{d,r} = \frac{\sum_l VKT_{d,r,l}}{\sum_r \sum_l VKT_{d,r,l}} \quad (14)$$

$$389 \quad \omega_{d,l} = \frac{VKT_{d,r,l}}{\sum_r \sum_l VKT_{d,r,l}} \quad (15)$$

390 **3 CARS Configuration**

391 The CARS model is an open-source program based on Python (Guido van Rossum, 2009)
392 that allows the users to efficiently apply open-source modules to develop programs. Users can
393 easily install Python development tools and load customized packages and modules to set up the
394 CARS development environment. All CARS modules are developed using Python v3.6. Other than
395 the GIS road shapefiles, all input files are based in the ASCII CSV format, which can be easily
396 handled by both spreadsheet programs and programming languages, making it more accessible for
397 users of all skillsets. The CARS can not only estimate district-level and spatially enhanced road
398 link-level emissions, but can also generate hourly chemically speciated gridded emissions for
399 CTMs. In addition, the CARS also generates various summary reports, graphics, and
400 georeferenced plots for quality assurance.

401 The required Python modules for the CARS are: “*geopandas*,” “*shapely.geometry*,” and
402 “*csv*” modules to read the shapefiles and table data files. The “*NumPy*” and “*pandas*” modules
403 are used to operate the memory arrays and scientific calculations while the “*pyproj*” module deals
404 with converting the projection coordinate systems. “*matplotlib*” is for generating any type of
405 figures/plots. Furthermore, the CARS model can also read and write Climate and Forecast (CF)-
406 compliant NetCDF-formatted files using “*NetCDF4*”.

407 The first process in the CARS is “*Loading_function_path*”; it allows users to define and
408 check the input file paths. Once all input files are checked, there are six process modules in CARS
409 to process inputs, compute emissions, and generate various output files, including QA reports.



410 Figure 5 is the schematic of the CARS that consists of six process modules with various functions.
411 The six process modules are (1) “**Process activity data**”, (2) “**Process emission factors**”, (3)
412 “**Process shapefile**”, (4) “**Calculate district emissions**”, (5) “**Grid4AQM**”, and (6) “**Plot figures**”.
413 The main purpose of modularizing the CARS is to meet the needs of various communities, such
414 as policymakers, stakeholders, and air quality modelers. While modules (1) through (4) are
415 required to develop the district-level and road link-level emissions inventories, module (5)
416 “**Grid4AQM**” is optional depending on if users want to develop chemically-speciated gridded
417 hourly emissions for CTMs. Also, the modularity system in the CARS allows users to bypass
418 certain modules if it has been previously processed without any changes. For example, if there is
419 no change in traffic activity, emission factors table, or GIS shapefiles, users do not need to run
420 these modules and can simply read the data frame outputs and then run “**Grid4AQM**” for the
421 modeling dates and domain. The “**Grid4AQM**” module will not only improve the computational
422 time for CTMs but also eliminate the need for a 3rd party emissions modeling system like SMOKE
423 (Baek and Seppanen, 2021).

424 The rectangle boxes in Fig. 5 represent the data array and the boxes with rounded edges are
425 the functions in the CARS. Details on the CARS code, input table format, and functions setup
426 information can be found on the CARS GitHub website (Pedruzzi *et al.*, 2020).

427 The “**Process activity data**” module first reads the vehicle activity data, such as an
428 individual vehicle's daily total VKT based on its registered district. The “**Process emission factors**”
429 module reads and stores the emission factors table that holds all pollutant emission factors to
430 estimate the emissions for all vehicles. Meteorology-sensitive emission factors are only limited to
431 NO_x pollutants. District boundary GIS shapefiles and road network shapefiles are processed
432 through “**Process shape file**” to generate the VKT-based redistribution weighting factors from Eq.
433 (13), (14) and (15) for the “**Calculate district emissions**” module to compute district-level and
434 road link-level emission rates (metric tons per year, t yr⁻¹).

435 The redistributed emission rates (t yr⁻¹) from the “**Calculate district emissions**” module
436 present annual total emission rates until district-level VKTs from the “**Process activity data**”
437 module are added. Then, the “**Grid4AQM**” module can generate CTM-ready chemically speciated
438 emissions. The “**Read_chemical**” function from the “**Grid4AQM**” module is designed to process
439 the chemical speciation profile that can convert the inventory pollutants such as CO, NO_x, SO₂,
440 PM₁₀, PM_{2.5}, VOC, and NH₃, into the chemically lumped model species that CTM requires for
441 chemical mechanisms, such as SAPRC (L. and Heo, 2012) and Carbon Bond version 6 (CB6)
442 (Yarwood and Jung, 2010). The “**Read_temporal**” function processes the complete set of monthly,
443 weekly, and hourly temporal allocation profiles that can convert annual total emissions to hourly
444 emissions. “**Read_griddesc**” defines the CTM-ready modeling domain and computes the gridding
445 fractions for all road link-level emissions by overlaying the modeling domain over the GIS
446 shapefiles. Once annual total emissions are chemically speciated, spatially gridded, and temporally
447 allocated into hourly emissions, the “**Gridded_emis**” function will combine emission source-level



448 conversion fractions from each function (*Read_chemical*, *Read_temporal*, and *Read_griddesc*) to
449 generate the CTM-ready chemically speciated, gridded hourly emissions in the NetCDF binary
450 format. The “**Plot Figures**” module is designed for generating various summary reports and
451 graphics to assist users in understanding the estimated automobile emissions inventory computed
452 by the CARS. The following section will describe the detailed processes of the “**Grid4AQM**”
453 module, which includes chemical, spatial, and temporal allocations.

454 **3.1 Chemical Speciation**

455 To support CTMs applications, the CARS needs to be able to convert inventory pollutants
456 into chemical lumped model species based on the choice of CTM chemical mechanisms. NO_x
457 includes nitric oxide (NO), nitrogen dioxide (NO_2), and nitrous acid (HONO). VOCs can represent
458 hundreds of different organic carbon species, such as benzene, acetaldehyde, and formaldehyde.
459 These grouped inventory pollutants cannot be directly imported into the chemical mechanism
460 modules in the CTM system and require chemical speciation allocation for CTMs to process them
461 during their chemical reactions. Therefore, the “**Grid4AQM**” module performs the chemical
462 species allocation step prior to the temporal and spatial allocations to generate the gridded hourly
463 emissions. The “*Read_chemical*” function in “**Grid4AQM**” module allows users to assign these
464 emission inventory pollutants to CTM-ready surrogate chemical species (a.k.a lumped chemical
465 species) by vehicle, engine, and fuel type. For example, VOC emissions from diesel busses can be
466 converted into the following composition based on its chemical allocation profile: alkanes (68%),
467 toluene (9%), xylenes (8%), alkenes (4%), ethylene (2%), benzene (1.3%), and unreactive
468 compounds (7%) when CB6 chemical mechanism is selected. Further details on the chemical
469 speciation profile input formats are available in the CARS user’s guide.

470 **3.2 Spatial Allocation**

471 The “**Calculate district emissions**” module calculates not only the total district emissions
472 but also road link-specific emissions based on road link-specific AADT data from road network
473 GIS shapefiles. The “**Calculate district emissions**” module first gets the district total vehicle
474 emissions (Eq. 2) based on the district-level VKTs, and then the normalized district total emissions
475 by district weight factor, ω_d (Eq. 13). Afterwards, the normalized district total emissions are
476 redistributed into every road link using road link-level weight factors ($\omega_{d,l}$) (Eq. 15). The district
477 total emissions from Eq. (2) and from Eq. (15) remain the same. Then the computed road link-
478 level emissions then will be converted into grid cell emissions using the modeling domain grid cell
479 fractions computed in the “*Read_griddesc*” function in the “**Grid4AQM**” module.



480 3.3 Temporal Allocation

481 Once chemical and spatial allocations are completed, the final step to support CTM
482 application is a temporal allocation that converts the annual total emissions from the “**Calculate**
483 **district emissions**” module into hourly emissions. The “*Read_temporal*” temporal allocation
484 function in the “**Grid4AQM**” module converts the annual emission rate (t yr^{-1}) to the hourly
485 emission rate (mol hr^{-1}) using monthly, weekly, and weekday/weekend diurnal temporal profiles.
486 This module processes these temporal profile inputs, which are the monthly (January - December),
487 weekly (Monday - Sunday), and weekday/weekend 24 hour profile tables (0:00-23:00 LST). The
488 users can assign these temporal profiles with a combination of vehicle, engine, fuel, and road types
489 to enhance their temporal representations in detail.

490 3.4 Chemical Transport Model Emissions

491 The main goal of the “**Grid4AQM**” module is to generate temporally, chemically, and
492 spatially enhanced CTM-ready gridded hourly emissions. First, it reads the CTM modeling domain
493 configuration and then overlays it over the road network GIS shapefile and district-boundary
494 shapefile to define the modeling domain. This overlaying process between the road network,
495 district boundary GIS shapefiles, and modeling domain allows the “**Grid4AQM**” module to
496 compute the fraction of road links that intersects with each grid cell. Figure 6 demonstrates how
497 the district boundary and road network GIS shapefiles are used to perform the spatial allocation
498 processes in CARS. Figure 6a is a native road link shapefile of Seoul with AADT, VKT, district
499 ID, and road type. Figure 6b presents an overlay of two districts’s road links (purple and blue)
500 over the selected region. State total emissions will be renormalized into weighed district total
501 emission data and then redistributed into the road link. Figure 6c illustrates how the weighted road
502 link-level emissions get allocated into modeling grid cells for CTMs. The link-level VKT ($VKT_{d,r,l}$)
503 from Eq. (12) will be used to compute a total of traffic activity fractions by grid cell and then use
504 that to assign the link-level emissions from Eq. (2) into each grid cell. When a road link intersects
505 with multiple grid cells, the “**Grid4AQM**” module will weigh the emissions by the length of the
506 link that intersects with each grid cell.

507 Through the overlay process, the CARS model can generate various types of output data,
508 such as total district emissions, link-level emissions, and CTM-ready gridded emissions. For
509 example, the CO vehicle emissions from the Seoul metropolitan in South Korea are presented in
510 three different output formats in Fig. 7. Figure 7a shows the annual mobile PM_{2.5} emissions by
511 district. The road link level annual emissions are presented in Fig. 7b. Furthermore, the CARS
512 applies the link-level emissions from Fig. 7b to generate the hourly grid cell emission data with a
513 1 km × 1 km resolution for the CTM in Fig. 7c.



514 3.5 National Control Strategy Application

515 One of the unique features in the CARS compared to other mobile emissions models is that
516 it can promptly develop controlled mobile emissions responding to the national emergency high
517 PM_{2.5} episodes. It is very common to experience high PM_{2.5} episodes, especially during the
518 wintertime in South Korea due to domestic and international primary and secondary air pollutants
519 emissions. When the 72 hour forecasted PM_{2.5} concentration exceeds the average 50 µg/m³ (0:00-
520 16:00 LST), the national PM_{2.5} emergency control strategy is activated for ten days. It applies a
521 nationwide vehicle restriction policy within 24 hours. It enforces a limit on what kind of vehicles
522 can be operated on a certain date. The restrictions can be applied in the following ways: the
523 closures of public parks and government facilities, and restrictions of certain vehicles based on
524 their fuel type and age, which is a major factor of engine deterioration. This policy will limit the
525 number of vehicles on the network roads significantly, which could reduce primary PM_{2.5} and
526 precursor pollutant (NO_x, NH₃, and VOC) emissions, especially from heavily populated
527 metropolitan regions (Choi et al., 2014; Kim et al., 2017a; Kim et al., 2017b; Kim et al., 2017c).

528 To understand the impacts of an even/odd vehicle restriction policy in real-time, we need to
529 quickly develop a rapid control response emissions for the air quality forecast modeling system.
530 The process of generating the controlled mobile emissions can take a long time if we start fresh.
531 Thus, we have implemented this control strategy as an optional “**Control Factors**” function in the
532 “**Calculate district emissions**” in the module for users to quickly and easily generate the
533 controlled mobile emissions with consideration of the limited number of vehicles based on the
534 vehicle, engine, fuel, and vehicle manufactured year. A one hundred percent (100%) control factor
535 means that there are no emissions from those selected vehicles.

536 Because of the modularization system in the CARS, we can bypass some computationally
537 expensive data processing modules (i.e., “**Process activity data**”, “**Process emission factors**”,
538 and “**Process shape file**”) and let the “**Calculate district emissions**” module quickly apply control
539 factors while it computes the district-level mobile emission inventory from Eq. (2). This will allow
540 users to reduce the computational time to generate the controlled mobile emissions under a specific
541 control scenario and develop the controlled CTM-ready gridded hourly emissions using the
542 “**Grid4AQM**” module.

543 3.6 Computational Time

544 While the CARS can generate a high-quality spatiotemporal emission inventory for
545 policymakers, stakeholders, and air quality modelers, it is quite critical for the CARS to generate
546 these complex mobile emissions effectively and accurately without being at the expense of
547 computational time. This is especially important to meet the needs for an air quality forecast
548 modeling system responding to a national emergency control strategy implementation.



549 In this section, we will discuss the details of the CARS computational modeling performance.
550 While the CARS model has been highly optimized, the modularization of CARS has also improved
551 its modeling performance with optional module runs. The breakdown of module-specific
552 computational time estimates based on the benchmark CARS runs are listed in Table 1. The
553 benchmark CARS case includes a total of 24,383,578 daily VKT datasets from KSTA over two
554 different years, 84,608 emission factors for all pollutants across a combination of vehicle-age-
555 engine-fuel types, 385,795 road links from the GIS road network shapefiles, 5,150 districts/16-
556 states boundary GIS shapefile, and 5,494 grid cells (=82 rows and 67 columns) for CTMs. Without
557 any computational parallelization, the total processing time of all six modules usually takes around
558 a half hour to generate a single day CTM-ready gridded hourly emission file. However, it can be
559 further shortened to 25-30 minutes on a higher performance computer. Because of the modular
560 system implemented in the CARS, generating one month (31 days) long gridded hourly emissions
561 from CTMs do not require over 15 computational hours, but only around 100 minutes on high-
562 performance computers. The maximum usage of RAM can reach up to 11 GB. Table 1 shows the
563 breakdown of computational time by each module from two different hardwares (desktop and
564 laptop computers). The numbers in parentheses beside the “Grid4AQM” module is the
565 computational time for a single day versus 31 days. While the “Grid4AQM” module takes an
566 average of 4.9 minutes for a single day emissions generation, processing a consecutive 31 days
567 saves 46% more time, decreasing from 151.9 minutes (=4.9 minutes * 31 days) to 81.6 minutes.

568 4 Results

569 CARS and CAPSS Comparison

570 The CARS model calculates the 2015 onroad automobile emissions based on the latest
571 2015 emission factors and the 2015-2017 vehicle activity database in South Korea. The annual
572 total emissions from CARS are compared against the ones from NIER CAPSS in Table 2. The
573 CARS model estimated the following annual total emissions in units of metric tons per year (t yr^{-1}):
574 NO_x (301,794); VOC (61,186); CO (373,864), NH_3 (12,453); $\text{PM}_{2.5}$ (10,108), and SO_x (172.0).
575 Compared to NIER CAPSS, the CARS overestimated all pollutants except for NO_x (-18% decrease)
576 and SO_x (-17% decrease). It overestimated the emissions of VOC by 33%, $\text{PM}_{2.5}$ by 15%, CO by
577 52%, and NH_3 by 24%. Both NIER CAPSS and CARS shared the same emission factor tables,
578 which hold over 84,608 emission factors for all pollutants across a combination of vehicle, age,
579 engine, and fuel types.

580 The difference between CAPSS and CARS approaches are caused by three reasons: First,
581 the number of vehicles used in CARS is slightly higher (6%) than CAPSS data (1.3 out of 23
582 million), as well as other key traffic-related activity inputs (i.e., vehicle age distribution, averaged
583 speed distribution, etc). Secondly, the vehicle speed information assigned by vehicle and road type
584 play a critical role in the differences between CAPSS and CARS. The CAPSS calculation was



585 based on the road-specific mean speed value or 80% of the speed limit as an input of vehicle
586 operating speed by three road types (rural, urban, and expressway). In other words, CAPSS only
587 assigns a “single-speed value” for each road type, and does not encounter the variation of vehicle
588 speed during its operation on roads into the emissions calculation. Most running exhaust emissions
589 occur during a vehicle’s low-speed operation due to its incomplete combustion of fuel, and it is
590 critical to accurately represent the emissions across various speed bins in order to compute the
591 correct emissions. The CARS model has an option to apply the average speed distribution (ASD)
592 over 16 speed bins for eight road types (Fig. 4). The CARS speed distribution process can better
593 represent the speed variations of vehicle speeds for each road type. A detailed analysis of the
594 impact of vehicle speed will be discussed later in this chapter. Lastly, other advanced processes in
595 the CARS, such as link-level AADT and district-level vehicle data (5,150 districts in South Korea),
596 can reflect more spatial detail and variation than the CAPSS. The CAPSS only considers state-
597 level data (17 states in South Korea) and five road types (interstate expressway, urban highway,
598 rural highway, urban local, and rural local).

599 Figure 8 illustrates more details about the difference between the annual emissions from
600 CARS to the CAPSS by pollutants and vehicle types. Sedan vehicles show the largest increase of
601 VOC (33%), CO (41%), and NH₃ (23%) in the CARS relative to CAPSS because almost 56% of
602 total vehicle count (13.5 million) is composed of sedan vehicles. Also, sedan vehicles contribute
603 51% of total VOC and 61% of total CO annual emissions. The VOC and CO emissions from sedans
604 are largely affected by the average speed distribution process when compared to other vehicle
605 types. Similarly, the largest decreases of NO_x (-16%) and SO_x (-18%) are from trucks because they
606 are significant NO_x (~50%) and SO_x contributors (~27%) and their emission factors are sensitive
607 to vehicle speed.

608 Onroad Emissions Analysis

609 The CARS is a bottom-up emissions model, which utilizes local individual vehicle activity
610 data, detailed local emission factors for every vehicle and fuel type, and localized inputs such as
611 average speed distribution by road type and deterioration factor. It allows users to assess the
612 detailed breakdown of localized emission contributions. Table 3 represents the individual air
613 pollutants (NO_x, VOC, PM_{2.5}, CO, NH₃, and SO_x) emission contributions (t yr⁻¹), fractions (%),
614 and impact factors (IF) by the vehicle type and fuel system. The IF is defined by the normalized
615 annual emissions with vehicle counts of each category (kg yr⁻¹ per vehicle). The CARS also can
616 provide the average daily VKT per vehicle, which is the total daily VKT divided by vehicle
617 numbers, to explain the emission contributions in Appendix D.

618 Diesel-fueled vehicles contribute the most of NO_x emissions, which is over 85.3% (257,305
619 t yr⁻¹), although the number of diesel vehicles only amounts to approximately 35% of the total
620 vehicles (Table 3a). While the diesel trucks emitted 49.1% (148,246 t yr⁻¹) of total NO_x with an IF



621 value of $47.9 \text{ (kg yr}^{-1}\text{)}$, the highest impact ($\text{IF} = 340 \text{ kg yr}^{-1}$) occurred from diesel buses with only
622 a 8.51% contribution to the total NO_x emissions. This is caused by the highest average daily VKT
623 from diesel buses compared to other vehicles, which is expected in a highly populated metropolitan
624 area like Seoul, South Korea. A diesel bus generally has a 3-5 times higher daily VKT (180 km d^{-1}
625 1) than other common vehicles (gasoline sedan: 34 km d^{-1} , diesel truck: 57 km d^{-1}). The second-
626 largest vehicle type is the CNG (compressed natural gas) bus (248 kg yr^{-1}), which also has a higher
627 VKT. Their average daily VKT is 212 km d^{-1} , with only a 3.1% NO_x contribution.

628 For VOC emissions, over 12 million gasoline vehicles cause 52.1% ($31,885 \text{ t yr}^{-1}$) of the
629 total VOC emissions, and the gasoline sedan is the highest contributor across all vehicle types,
630 which is over $28,434 \text{ t yr}^{-1}$ (46.5%) (Table 3b). Unlike NO_x emissions, diesel vehicles only
631 contribute 23.0% ($14,070 \text{ t yr}^{-1}$) of the total VOC emissions. Across the vehicle fuel types, the IF
632 outcome indicates that CNG vehicles have the highest IF values for VOC, which is 247 kg yr^{-1} due
633 to the relatively high VOC contribution (19% over total VOC) and a low number of heavy CNG
634 vehicles. The IF of CNG trucks are 77.2 kg yr^{-1} , but only contribute 0.2% to total VOC emissions.
635 The IF of the CNG bus is 320 kg yr^{-1} and emits 19.5% of the total VOC. Comparing the IFs of
636 buses across fuel types, the CNG bus emits less NO_x but higher VOC than a diesel vehicle. Each
637 CNG bus has about 33 times higher IF of VOC (320 kg yr^{-1}) than a diesel bus (9.51 kg yr^{-1}), and
638 CNG buses released slightly lower NO_x (248 kg yr^{-1}) than diesel buses (340 kg yr^{-1}) (Table 3a and
639 3b). It indicates that a CNG bus is better for rural areas and a diesel bus is better for urban areas to
640 control ozone, because the rural area is usually NO_x limited for ozone formation and urban areas
641 are VOC limited.

642 The current South Korea CAPSS onroad emissions inventory does not consider the $\text{PM}_{2.5}$
643 emissions from tire and brake wear, which are the highest contributors of $\text{PM}_{2.5}$ emissions from
644 vehicles on roads. For that reason, diesel vehicles become the major source of $\text{PM}_{2.5}$ emissions,
645 which contributes over 98.5% ($9,959 \text{ t yr}^{-1}$) of the $\text{PM}_{2.5}$ emissions based on the CARS 2015
646 emissions (Table 3c). The diesel truck, SUV, and van are the three major sources, and their
647 contributions of total $\text{PM}_{2.5}$ are 53.6%, 21.4%, and 11.2%, respectively. Although over 52% of the
648 vehicles are gasoline vehicles, their primary $\text{PM}_{2.5}$ contribution is limited to 1.44%. The diesel
649 bus has the highest IF (2.83 kg yr^{-1}), which is caused by the largest average daily VKTs.

650 Similar to VOC emissions, CO is mostly emitted through the tailpipe due to incomplete
651 internal combustion of fuel and share similar emissions distributions across vehicle and fuel types
652 (Table 3d). Gasoline vehicles contribute most of the CO ($220,390 \text{ t yr}^{-1}$, 59.0%), and sedan vehicles
653 are the primary source ($178,121 \text{ t yr}^{-1}$, 47.6%) of this out of all gasoline vehicles. Across vehicle
654 types, bus shows the highest IF of CO (81.2 kg yr^{-1}) due to its largest daily VKT. CO is the most
655 abundant pollutant released from vehicles ($373,864 \text{ t yr}^{-1}$) across all pollutants from onroad
656 automobile sources. Although CO is much less reactive than other vehicle VOCs (Rinke and
657 Zetzsch, 1984; Liu and Sander, 2015), the majority of CO emissions from onroad automobile
658 sources plays a critical role in generating 30% of hydroperoxyl radicals (HO_2) and causing ozone



659 formation in urban areas (Pfister et al., 2019). Thus, CO is also another crucial precursor to ozone
660 formation in urban areas.

661 SO_x emissions are related to the sulfur content within the fuel component; diesel has a
662 higher sulfur content than any other fuels. Most SO_x is contributed by diesel vehicles (93.8 t yr⁻¹,
663 54.5%) (Table 3e). Within diesel vehicles, trucks provide 26.5% of SO_x (45. t yr⁻¹). Although the
664 SO_x from sedan vehicles are slightly higher (~3.3%) than diesel trucks, the number of diesel trucks
665 is only 29.6% of the number of gasoline sedans. Thus, diesel trucks have a higher IF than gasoline
666 sedans. Across vehicle types, buses have the highest IF (0.095 kg yr⁻¹) of SO_x, and diesel buses in
667 particular have the largest IF at 0.143 kg yr⁻¹.

668 The NH₃ emissions table (table 3f) indicates that 98.7% of NH₃ is from gasoline vehicles
669 while diesel trucks only contribute 1.13%. The IF result also shows that the gasoline sedan has the
670 most significant impact per vehicle (1.17 kg yr⁻¹).

671 According to the vehicle activity and the CARS model results, nearly half of the total
672 vehicles (24.3 million) are gasoline sedans (10.4 million, 42.8%), and gasoline sedan vehicles
673 contributed most of the VOC and CO emissions (46.5% and 47.6%), but only 7.7% of the total
674 NO_x emissions. The number of diesel vehicles is 8.6 million (35.4%); however, they emitted about
675 85.3% of the total NO_x and 98.5% of the primary PM_{2.5}. These results indicated that the annual
676 traffic-related mobile emissions are not only affected by the number of vehicles, but also by
677 different vehicle and fuel types. Therefore, this study normalized the annual emissions by the
678 number of vehicles to confirm the emission composition by individual vehicle types.

679 **Average Speed Impact Study**

680 The CARS can also optionally apply the average speed distribution (ASD) by road type to
681 compute more realistic mobile emissions on the road network when compared to using a current
682 single average speed value for each road type (Appendix E). Applying the ASD will generate a
683 much better representation of actual traffic patterns from each road type. To understand the impacts
684 of ASD application, we performed sensitivity runs between using a single-speed to the ASD
685 application (Appendix F). The ASD data was described in Fig. 4, and the road-specific average
686 single-speed values were developed based on the weighted average method using the same ASD
687 data. Appendix E and S6 describes the details of ASD as well as road-specific speed values.

688 Figure 9a shows the differences in total emissions between two scenarios and is organized
689 by pollutant. The single-speed scenario largely underestimates the emissions across all pollutants
690 compared to the ones from the ASD scenario. NO_x (16%), VOC (40%), and CO (30%) were
691 especially underestimated. The difference is caused by the lack of low-speed bins (<16 km h⁻¹)
692 representation when a single average speed approach was used. Higher emissions are emitted while
693 vehicles are operated with low-speed bins, which decreases the combustion efficiency of ICE and
694 releases more pollutants.



695 Figure 9b shows the road-specific breakdown between the ASD and single speed scenarios
696 to understand the impacts of vehicle operating speeds on onroad automobile emissions. In this
697 figure, each color indicates the emissions percentage differences by road types. Other than NH₃,
698 significant discrepancies happened between local urban roads (5.8%), highways (3.9%), and urban
699 highways (3.0%). Other pollutants, VOC, PM_{2.5}, CO, and SO_x, have similar fractions of road types.
700 This phenomenon is caused by low-speed conditions (<16 km h⁻¹) and the fractions of road VKT
701 contributions (Appendix C). The lower speeds cause the incomplete combustion of ICE and
702 increase the emission rate. Also, local urban roads, highways, and urban highways have higher
703 road VKT contributions at 17%, 18%, and 12%, respectively (Appendix C) than rural roads.
704 Higher emissions from low speed conditions from these high contribution roads (urban local, urban
705 highway, and highway) caused these significant differences between the ASD and single-speed
706 approaches. Although the interstate expressway has the largest VKT contribution (41%), it also
707 has the lowest fraction of low-speed bins (2%). That is why the difference between the ASD and
708 single speed scenarios on interstate expressways is less than 1%. In general, NH₃ emission factors
709 do not change by vehicle operating speed, so the ASD impact is quite minimal.

710 5 Conclusions

711 The CARS is a bottom-up automobile emissions model that utilizes the localized traffic-
712 related activity and emission factors input datasets to generate high quality localized bottom-up
713 emissions inventories for policymakers, stakeholders, and research community as well as
714 temporally and spatially enhanced hourly gridded emissions for CTMs. First, the CARS model
715 employs the daily VKTs for all registered vehicles and the emission factors function to compute
716 district-level total daily emissions for each vehicle. To reflect realistic traffic patterns, the CARS
717 model computes and utilizes link-level VKTs (=link-length×AADT) from the road network GIS
718 shapefiles to redistribute the original district-level total emissions into spatially enhanced road
719 link-level emissions. It can also optionally implement a control strategy as well as road restriction
720 rules to improve the quality of local emission inventories and meet the needs of users.

721 The CARS model is a fully modularized and computationally optimized python-based
722 bottom-up mobile emissions model that can effectively process a huge dataset to calculate high
723 quality spatiotemporal county-level, road link-level and grid cell-level mobile emissions. We
724 believe that the implementation of the ASD into the CARS improves the representation of onroad
725 automobile emissions from the road network when compared to a single-speed for each road type
726 approach. It allows the CARS to have a better representation of low speed (<16 km h⁻¹) vehicle
727 emissions. We believe that CARS model's versatile spatiotemporal bottom-up automobile
728 emissions and the in-depth analysis feature can assist government policymakers and stakeholders
729 to develop the rapid responsive emission abatement strategies as a response to the South Korea's
730 national PM_{2.5} emergency control strategy that enforces the nationwide vehicle restriction policy
731 within 24 hours.



732 **Code Availability:**

733 The source code of the CARS model public release version 1.0 can be downloaded from the
734 Github release website:

735 <https://github.com/bokhaeng/CARS/releases/tag/CARSv1.0>

736

737

738 **Digital Object Identifier (DOI) for the CARS version 1.0:**

739 <https://zenodo.org/record/5033314#.YNzDrC1h001>

740

741

742 **Installation Package for CARS version 1.0:**

743 The CARS version 1.0 installation package comes with the complete inputs and outputs datasets
744 for users to confirm their proper installation on their computers and can be downloaded from the
745 Github release website:

746 https://github.com/bokhaeng/CARS/releases/download/CARSv1.0/CARS_v1.0_public_release_package_25June2021.zip

747

748

749

750 **User's Guide Documentation:**

751 The CARS version user's guide documentation can be accessed through the Github repository:

752 https://github.com/bokhaeng/CARS/tree/master/docs/User_Manual

753

754

755 **Data availability:**

756 All the datasets, excel and python scripts used in this manuscript for the data analysis are
757 uploaded through GMD website along with a supplemental appendix document.

758

759 **Author contribution**

760 Dr. B.H. Baek and Dr. Jung-Hun Woo are lead researchers in this study. Dr. Rizzieri Pedruzzi
761 develop the source code of CARS model, Dr. Minwoo Park tested the model and provided the
762 model input data. Dr. Chi-Tsan Wang analyzed the model result and prepared the manuscript.
763 Younha Kim, Chul-Han Song, analyzed the model result and provided comments.

764

765



766 **Competing interests**

767 The Authors declare that they have no conflict of interest.

768 **Acknowledgments**

769 This research was funded by the National Strategic Project-Fine Particle of the National Research
770 Foundation (NRF) of Korea funded by the Ministry of Science and ICT (MSIT), the Ministry of
771 Environment (ME), the Ministry of Health and Welfare (MOHW) (NRF-2017M3D8A1092022),
772 and by the Korea Environmental Industry & Technology Institute (KEITI) through the Public
773 Technology Program based on Environmental Policy Program, funded by Korea Ministry of
774 Environment (MOE) (2019000160007).

775



776 References

- 777 Safety flare for burning combustible gas - has tangential inlet for non-flammable gas between
778 housing and stack, in, Shell Oil Co (Shel-C).
- 779 Anaconda, Anaconda python: <https://www.anaconda.com/products/individual>, last access: May,
780 1st, 2020.
- 781 Appel, W., Chemel, C., Roselle, S., Francis, X., Hu, R.-M., Sokhi, R., Rao, S. T., and Galmarini,
782 S.: Examination of the Community Multiscale Air Quality (CMAQ) model performance over the
783 North American and European domains, *Atmospheric Environment*, 53, 142–155,
784 10.1016/j.atmosenv.2011.11.016, 2013.
- 785 Baek, B. H., and Seppanen, C., SMOKE v4.8.1 Public Release (January 29, 2021) (Version
786 SMOKEv481_Jan2021): <http://doi.org/10.5281/zenodo.4480334> last 2021.
- 787 Choi, D., Beardsley, M., Brzezinski, D., Koupal, J., and Warila, J.: MOVES Sensitivity
788 Analysis: The Impacts of Temperature and Humidity on Emissions
789 , available at: <https://www3.epa.gov/ttn/chief/conference/ei19/session6/choi.pdf> 2017.
- 790 Choi, K.-C., Lee, J.-J., Bae, C. H., Kim, C.-H., Kim, S., Chang, L.-S., Ban, S.-J., Lee, S.-J., Kim,
791 J., and Woo, J.-H.: Assessment of transboundary ozone contribution toward South Korea using
792 multiple source–receptor modeling techniques, *Atmospheric Environment*, 92, 118-129,
793 <https://doi.org/10.1016/j.atmosenv.2014.03.055>, 2014.
- 794 Dennis, R., Fox, T., Fuentes, M., Gilliland, A., Hanna, S., Hogrefe, C., Irwin, J., Rao, S. T.,
795 Scheffe, R., Schere, K., Steyn, D., and Venkatram, A.: A FRAMEWORK FOR EVALUATING
796 REGIONAL-SCALE NUMERICAL PHOTOCHEMICAL MODELING SYSTEMS, *Environ*
797 *Fluid Mech (Dordr)*, 10, 471-489, 10.1007/s10652-009-9163-2, 2010.
- 798 EEA: EMEP/EEO air pollutant emission inventory guidebook 2016, 2019.
- 799 Enthought, Enthought Canapy Python: <https://assets.enthought.com/downloads/edm/>, last
800 access: May, 1st, 2020.
- 801 Fallahshorshani, M., André, M., Bonhomme, C., and Seigneur, C.: Coupling Traffic, Pollutant
802 Emission, Air and Water Quality Models: Technical Review and Perspectives, *Procedia - Social*
803 *and Behavioral Sciences*, 48, 1794-1804, <https://doi.org/10.1016/j.sbspro.2012.06.1154>, 2012.



- 804 Guevara, M., Tena, C., Porquet, M., Jorba, O., and Pérez García-Pando, C.: HERMESv3, a
805 stand-alone multi-scale atmospheric emission modelling framework – Part 1: global and regional
806 module, *Geosci. Model Dev.*, 12, 1885-1907, 10.5194/gmd-12-1885-2019, 2019.
- 807 Hogrefe, C., Rao, S. T., Kasibhatla, P., Hao, W., Sistla, G., Mathur, R., and McHenry, J.:
808 Evaluating the performance of regional-scale photochemical modeling systems: Part II—ozone
809 predictions, *Atmospheric Environment*, 35, 4175-4188, [https://doi.org/10.1016/S1352-](https://doi.org/10.1016/S1352-2310(01)00183-2)
810 [2310\(01\)00183-2](https://doi.org/10.1016/S1352-2310(01)00183-2), 2001a.
- 811 Hogrefe, C., Rao, S. T., Kasibhatla, P., Kallos, G., Tremback, C. J., Hao, W., Olerud, D., Xiu,
812 A., McHenry, J., and Alapaty, K.: Evaluating the performance of regional-scale photochemical
813 modeling systems: Part I—meteorological predictions, *Atmospheric Environment*, 35, 4159-
814 4174, [https://doi.org/10.1016/S1352-2310\(01\)00182-0](https://doi.org/10.1016/S1352-2310(01)00182-0), 2001b.
- 815 Ibarra-Espinosa, S., Ynoue, R., amp, apos, Sullivan, S., Pebesma, E., Andrade, M. d. F., and
816 Osses, M.: VEIN v0.2.2: an R package for bottom–up vehicular emissions inventories, *Geosci.*
817 *Model Dev.*, 11, 2209-2229, 10.5194/gmd-11-2209-2018, 2018a.
- 818 Ibarra-Espinosa, S., Ynoue, R., O'Sullivan, S., Pebesma, E., Andrade, M. D. F., and Osses, M.:
819 VEIN v0.2.2: an R package for bottom–up vehicular emissions inventories, *Geosci. Model Dev.*,
820 11, 2209-2229, 10.5194/gmd-11-2209-2018, 2018b.
- 821 IEMA, Inventário de Emissões Atmosféricas do Transporte Rodoviário de Passageiros no
822 Município de São Paulo.: <http://emissoes.energiaeambiente.org.br>, last access: May,1st, 2017.
- 823 Jang, Y. K., Cho, K. L., Kim, K., Kim, H. J., and Kim, J.: Development of methodology for
824 esimation of air pollutants emissions and future emissions from on-road mobile sources.,
825 National Institute of Environmental Research, Incheon, Korea., available at: 2007.
- 826 Kaewunruen, S., Sussman, J. M., and Matsumoto, A.: Grand Challenges in Transportation and
827 Transit Systems, *Frontiers in Built Environment*, 2, 10.3389/fbuil.2016.00004, 2016.
- 828 Kim, B.-U., Bae, C., Kim, H. C., Kim, E., and Kim, S.: Spatially and chemically resolved source
829 apportionment analysis: Case study of high particulate matter event, *Atmospheric Environment*,
830 162, 55-70, <https://doi.org/10.1016/j.atmosenv.2017.05.006>, 2017a.
- 831 Kim, H. C., Kim, E., Bae, C., Cho, J. H., Kim, B. U., and Kim, S.: Regional contributions to
832 particulate matter concentration in the Seoul metropolitan area, South Korea: seasonal variation



- 833 and sensitivity to meteorology and emissions inventory, *Atmos. Chem. Phys.*, 17, 10315-10332,
834 10.5194/acp-17-10315-2017, 2017b.
- 835 Kim, H. C., Kim, S., Kim, B.-U., Jin, C.-S., Hong, S., Park, R., Son, S.-W., Bae, C., Bae, M.,
836 Song, C.-K., and Stein, A.: Recent increase of surface particulate matter concentrations in the
837 Seoul Metropolitan Area, Korea, *Scientific Reports*, 7, 4710, 10.1038/s41598-017-05092-8,
838 2017c.
- 839 L., W. P., and Heo, G.: Development of revised SAPRC aromatics mechanism, available at:
840 <https://www.engr.ucr.edu/~carter/SAPRC/saprc11.pdf> 2012.
- 841 Lee, D., Lee, Y.-M., Jang, K.-W., Yoo, C., Kang, K.-H., Lee, J.-H., Jung, S.-W., Park, J.-M.,
842 Lee, S.-B., Han, J.-S., Hong, J.-H., and Lee, S.-J.: Korean National Emissions Inventory System
843 and 2007 Air Pollutant Emissions, *Asian Journal of Atmospheric Environment*, 5-4, 278-291,
844 2011a.
- 845 Lee, D.-G., Lee, Y.-M., Jang, K.-W., Yoo, C., Kang, K.-H., Lee, J.-H., Jung, S.-W., Park, J.-M.,
846 Lee, S.-B., Han, J.-S., Hong, J.-H., and Lee, S.-J.: Korean National Emissions Inventory System
847 and 2007 Air Pollutant Emissions, *Asian Journal of Atmospheric Environment*, 5,
848 10.5572/ajae.2011.5.4.278, 2011b.
- 849 Lejri, D., Can, A., Schiper, N., and Leclercq, L.: Accounting for traffic speed dynamics when
850 calculating COPERT and PHEM pollutant emissions at the urban scale, *Transportation Research*
851 *Part D: Transport and Environment*, 63, 588-603, <https://doi.org/10.1016/j.trd.2018.06.023>,
852 2018.
- 853 Li, F., Zhuang, J., Cheng, X., Li, M., Wang, J., and Yan, Z.: Investigation and Prediction of
854 Heavy-Duty Diesel Passenger Bus Emissions in Hainan Using a COPERT Model, *Atmosphere*,
855 10, 106, 10.3390/atmos10030106, 2019.
- 856 Li, Q., Qiao, F., and yu, L.: Vehicle Emission Implications of Drivers Smart Advisory System
857 for Traffic Operations in Work Zones, *Journal of the Air & Waste Management Association*, 11,
858 10.1080/10962247.2016.1140095, 2016.
- 859 Liu, H., Guensler, R., Lu, H., Xu, Y., Xu, X., and Rodgers, M.: MOVES-Matrix for High-
860 Performance On-Road Energy and Running Emission Rate Modeling Applications, *Journal of*
861 *the Air & Waste Management Association*, 69, 10.1080/10962247.2019.1640806, 2019.



- 862 Liu, Y., and Sander, S. P.: Rate Constant for the OH + CO Reaction at Low Temperatures, The
863 Journal of Physical Chemistry A, 119, 10060-10066, 10.1021/acs.jpca.5b07220, 2015.
- 864 Luo, H., Astitha, M., Hogrefe, C., Mathur, R., and Rao, S. T.: A new method for assessing the
865 efficacy of emission control strategies, Atmospheric Environment, 199, 233-243,
866 <https://doi.org/10.1016/j.atmosenv.2018.11.010>, 2019.
- 867 Lv, W., Hu, Y., Li, E., Liu, H., Pan, H., Ji, S., Hayat, T., Alsaedi, A., and Ahmad, B.: Evaluation
868 of vehicle emission in Yunnan province from 2003 to 2015, J. Clean Prod., 207, 814-825,
869 <https://doi.org/10.1016/j.jclepro.2018.09.227>, 2019.
- 870 Moussiopoulos, N., Vlachokostas, C., Tsilingiridis, G., Douros, I., Hourdakis, E., Naneris, C.,
871 and Sidiropoulos, C.: Air quality status in Greater Thessaloniki Area and the emission reductions
872 needed for attaining the EU air quality legislation, Sci. Total Environ., 407, 1268-1285,
873 <https://doi.org/10.1016/j.scitotenv.2008.10.034>, 2009.
- 874 Nagpure, A. S., Gurjar, B. R., Kumar, V., and Kumar, P.: Estimation of exhaust and non-exhaust
875 gaseous, particulate matter and air toxics emissions from on-road vehicles in Delhi, Atmospheric
876 Environment, 127, 118-124, 10.1016/j.atmosenv.2015.12.026, 2016.
- 877 NIER: Study on Air Pollutant Emission Estimation Method in Transportation section(II) 11-
878 1480523-003573-01, National Archives of Korea, available at:
879 [https://www.archives.go.kr/next/manager/publishmentSubscriptionDetail.do?prt_seq=114054&](https://www.archives.go.kr/next/manager/publishmentSubscriptionDetail.do?prt_seq=114054&page=1554&prt_arc_title=&prt_pub_kikwan=&prt_no)
880 [age=1554&prt_arc_title=&prt_pub_kikwan=&prt_no](https://www.archives.go.kr/next/manager/publishmentSubscriptionDetail.do?prt_seq=114054&page=1554&prt_arc_title=&prt_pub_kikwan=&prt_no) 2018.
- 881 Ntziachristos, L., and Samaras, Z.: Speed-dependent representative emission factors for catalyst
882 passenger cars and influencing parameters, Atmospheric Environment, 34, 4611-4619,
883 [https://doi.org/10.1016/S1352-2310\(00\)00180-1](https://doi.org/10.1016/S1352-2310(00)00180-1), 2000.
- 884 Ntziachristos, L., Gkatzoflias, D., Kouridis, C., and Samaras, Z.: COPERT: A European road
885 transport emission inventory model, 491-504 pp., 2009.
- 886 Pedruzzi, R., Baek, B. H., and Wang, C.-T., CARS: <https://github.com/CMASCenter/CARS>,
887 last access: MAy, 1st, 2020.
- 888 Perugu, H., Ramirez, L., and DaMassa, J.: Incorporating temperature effects in California's on-
889 road emission gridding process for air quality model inputs, Environ Pollut, 239, 1-12,
890 10.1016/j.envpol.2018.03.094, 2018.



- 891 Perugu, H.: Emission modelling of light-duty vehicles in India using the revamped VSP-based
892 MOVES model: The case study of Hyderabad, Transportation Research Part D: Transport and
893 Environment, 68, 150-163, <https://doi.org/10.1016/j.trd.2018.01.031>, 2019.
- 894 Pfister, G., Wang, C.-t., Barth, M., Flocke, F., Vizuete, W., and Walters, S.: Chemical
895 Characteristics and Ozone Production in the Northern Colorado Front Range, JGR, 2019.
- 896 Pinto, J. A., Kumar, P., Alonso, M. F., Andreão, W. L., Pedruzzi, R., dos Santos, F. S., Moreira,
897 D. M., and Albuquerque, T. T. d. A.: Traffic data in air quality modeling: A review of key
898 variables, improvements in results, open problems and challenges in current research,
899 Atmospheric Pollution Research, 11, 454-468, <https://doi.org/10.1016/j.apr.2019.11.018>, 2020.
- 900 Rao, S. T., Galmarini, S., and Puckett, K.: Air Quality Model Evaluation International Initiative
901 (AQMEII): Advancing the State of the Science in Regional Photochemical Modeling and Its
902 Applications, Bulletin of the American Meteorological Society, 92, 23-30,
903 10.1175/2010BAMS3069.1, 2011.
- 904 Rey DR, S. A., Guevara M, Linares MP Evaluation of traffic emission models coupled with a
905 microscopic traffic simulator and on-road measure, 2018.
- 906 Rinke, M., and Zetzsch, C.: Rate Constants for the Reactions of OH Radicals with Aromatics:
907 Benzene, Phenol, Aniline, and 1,2,4-Trichlorobenzene, Berichte der Bunsengesellschaft für
908 physikalische Chemie, 88, 55-62, 10.1002/bbpc.19840880114, 1984.
- 909 Russell, A., and Dennis, R.: NARSTO critical review of photochemical models and modeling,
910 Atmospheric Environment, 34, 2283-2324, [https://doi.org/10.1016/S1352-2310\(99\)00468-9](https://doi.org/10.1016/S1352-2310(99)00468-9),
911 2000.
- 912 Ryu, J. H., Han, J. S., Lim, C. S., Eom, M. D., Hwang, J. W., Yu, S. H., Lee, T. W., Yu, Y. S.,
913 and Kim, G. H.: The Study on the Estimation of Air Pollutants from Auto- mobiles (I) -
914 Emission Factor of Air Pollutants from Middle and Full sized Buses., in, Transportation
915 Pollution Research Center, National Institute of Environmental Research, Incheon, Korea., 2003.
- 916 Ryu, J. H., Lim, C. S., Yu, Y. S., Han, J. S., Kim, S. M., Hwang, J. W., Eom, M. D., Kim, G. Y.,
917 Jeon, M. S., Kim, Y. H., Lee, J. T., and Lim, Y. S.: The Study on the Esti- mation of Air
918 Pollutants from Automobiles (II) - Emis- sion Factor of Air Pollutants from Diesel Truck., in,
919 Trans- portation Pollution Research Center, National Institute of Environmental Research,
920 Incheon, Korea., 2004.



- 921 Ryu, J. H., Yu, Y. S., Lim, C. S., Kim, S. M., Kim, J. C., Gwon, S. I., Jeong, S. W., and Kim, D.
922 W.: The Study on the Estimation of Air Pollutants from Automobiles (III) - Emission Factor of
923 Air Pollutants from Small sized Light-duty Vehicles., in, Transportation Pollution Research
924 Center, National Institute of Environmental Research, Korea., 2005.
- 925 Sallis, P., Bull, F., Burdett, P., Frank, P., Griffiths, P., Giles-Corti, P., and Stevenson, M.: Use of
926 science to guide city planning policy and practice: How to achieve healthy and sustainable future
927 cities, *The Lancet*, 388, 10.1016/S0140-6736(16)30068-X, 2016.
- 928 Smit, R., Kingston, P., Neale, D. W., Brown, M. K., Verran, B., and Nolan, T.: Monitoring on-
929 road air quality and measuring vehicle emissions with remote sensing in an urban area,
930 *Atmospheric Environment*, 218, 116978, <https://doi.org/10.1016/j.atmosenv.2019.116978>, 2019.
- 931 Sun, W., Duan, N., Yao, R., Huang, J., and Hu, F.: Intelligent in-vehicle air quality
932 management : a smart mobility application dealing with air pollution in the traffic, 2016.
- 933 Tominaga, Y., and Stathopoulos, T.: Ten questions concerning modeling of near-field pollutant
934 dispersion in the built environment, *Build. Environ.*, 105, 390-402,
935 <https://doi.org/10.1016/j.buildenv.2016.06.027>, 2016.
- 936 USEPA: Population and Activity of Onroad Vehicles in MOVES3, in, edited by: USEPA, 2020.
- 937 WHO, Ambient air pollution- a major threat to health and climate:
938 <https://www.who.int/airpollution/ambient/en/>, last 2019.
- 939 Xu, X., Liu, H., Anderson, J. M., Xu, Y., Hunter, M. P., Rodgers, M. O., and Guensler, R. L.:
940 Estimating Project-Level Vehicle Emissions with Vissim and MOVES-Matrix, *Transportation*
941 *Research Record*, 2570, 107-117, 10.3141/2570-12, 2016.
- 942 Yarwood, G., and Jung, J.: UPDATES TO THE CARBON BOND MECHANISM FOR
943 VERSION 6 (CB6), 2010.
944



945 **Tables**

946 **Table 1.** Computational processing time by CARS module based on the modeling setup: Total
 947 number of activity data = 24,383,578; Emission Factors = 84,608; GIS road links=385,795;
 948 districts/states=5,150/16; 9km×9km grid cells=5,494 (82 columns× 67 columns).

No	Module	Desktop i7 (minutes)	Laptop i9 (minutes)	Averaged Time (minutes)
1	Process activity data	1.8	1.5	1.7
2	process emission factors	1.1	0.8	1.0
3	Process shape file	9.9	7.3	8.6
4	Calculate district emissions	6.4	5.7	6.1
5	Grid4AQM [31days]	4.8 [75.9]	5.0 [87.2]	4.9 [81.6]
6	Plot figures	6.2	5.4	5.8
Total [31days]		30.2 [101.3]	25.7 [107.9]	28.1[104.8]

949
 950
 951



952 **Table 2.** The total emissions comparison between CARS and CAPSS for the 2015 emission.

Emission Inventory	Pollutants (t yr ⁻¹)					
	NO _x	VOC	PM2.5	CO	SO _x	NH ₃
CARS 2015	301,794	61,186	10,108	373,864	172	12,453
CAPSS 2015	369,585	46,145	8,817	245,516	209	10,079

953

954



955 **Table 3.** The summary tables of emissions (t yr^{-1}), contributions (%), and impact factor (IF, kg yr^{-1})
 956 per vehicle for criteria air pollutants (CAPs) by vehicle and fuel types: (a) for NO_x ; (b) VOC;
 957 (c) for $\text{PM}_{2.5}$; (d) for CO; (e) for SO_x ; and (f) for NH_3 .

958
 959 (a) NO_x

Vehicle	Gasoline		Diesel		LPG		CNG		Hybrid		Total	
	Emission	IF	Emission	IF	Emission	IF	Emission	IF	Emission	IF	Emission	IF
Sedan	20,219 (6.70%)	1.94	14,783 (4.90%)	12.8	8,159 (2.77%)	4.49	12 (0.00%)	1.26	65 (0.02%)	0.39	43,239 (14.3%)	3.19
Truck	23 (0.01%)	5.54	148,246 (49.1%)	47.9	920 (0.31%)	4.55	88 (0.03%)	66.4	-	-	149,277 (49.5%)	45.2
Bus	0 (0.00%)	0.97	25,677 (8.51%)	340	-	-	9,260 (3.07%)	248	0 (0.00%)	1.77	34,938 (11.6%)	333
SUV	159 (0.05%)	1.19	39,565 (13.1%)	11.4	175 (0.06%)	8.54	0 (0.00%)	1.60	1 (0.00%)	0.42	39,900 (13.2%)	11.0
Van	14 (0.00%)	4.78	16,659 (5.52%)	22.6	1,337 (0.44%)	6.80	0 (0.00%)	1.25	0 (0.00)	0.37	18,012 (6.00%)	19.2
Taxi	-	-	-	-	1,217 (0.40%)	2.11	-	-	-	-	1,217 (0.40%)	2.11
Special	1 (0.00%)	20.1	12,347 (4.10%)	152	0 (0.00%)	0.52	-	-	-	-	12,375 (4.10%)	151
Motorcycle	2,836 (0.94%)	1.31	-	-	-	-	-	-	-	-	2,836 (0.94%)	1.32
Total	23,253 (7.70%)	1.83	257,305 (85.3%)	29.9	11,809 (3.91%)	4.20	9,361 (3.10%)	36.7	66 (0.02%)	0.39	301,794 (100%)	13.3

960
 961

(b) VOC

Vehicle	Gasoline		Diesel		LPG		CNG		Hybrid		Total	
	Emission	IF	Emission	IF	Emission	IF	Emission	IF	Emission	IF	Emission	IF
Sedan	28,434 (46.5%)	2.73	629 (1.03%)	0.55	2,107 (3.44%)	1.16	3 (0.01%)	0.33	77 (0.13%)	0.47	31,250 (51.1%)	2.30
Truck	23 (0.04%)	5.44	8,194 (13.4%)	2.65	286 (0.47%)	1.41	102 (0.17%)	77.2	-	-	8,605 (14.1%)	2.61
Bus	0 (0.00%)	1.65	717 (1.17%)	9.51	-	-	11,942 (19.5%)	320	0 (0.00%)	0	12,659 (20.7%)	112
SUV	246 (0.40%)	1.84	2,441 (3.99%)	0.71	46 (0.08%)	2.25	0 (0.00%)	0.75	1 (0.00%)	0.55	2,733 (4.47%)	0.76
Van	21 (0.03%)	7.04	1,185 (1.94%)	1.61	393 (0.64%)	2.00	0 (0.00%)	0.45	0 (0.00%)	0	1,599 (2.61%)	1.71
Taxi	-	-	-	-	273 (0.45%)	0.47	-	-	-	-	273 (0.45%)	0.47
Special	1 (0.00%)	25.8	904 (1.48%)	11.1	0 (0.00%)	0.23	-	-	-	-	905 (1.48%)	11.0
Motorcycle	3,160 (5.16%)	1.46	-	-	-	-	-	-	-	-	3,160 (5.16%)	1.46
Total	31,885 (52.1%)	2.50	14,070 (23.0%)	1.64	3,106 (5.08%)	1.10	12,047 (19.7%)	247	78 (0.13%)	0.47	61,186 (100%)	2.51

962
 963

(c) $\text{PM}_{2.5}$

Vehicle	Gasoline		Diesel		LPG		CNG		Hybrid		Total	
	Emission	IF	Emission	IF	Emission	IF	Emission	IF	Emission	IF	Emission	IF
Sedan	144 (1.42%)	0.01	809 (8.00%)	0.70	0	0	0	0	3 (0.03%)	0.02	956 (9.46%)	0.07
Truck	0 (0.01%)	0	5,415 (53.6%)	1.75	0	0	0	0	-	-	5,415 (53.6%)	1.64
Bus	0	0	214 (2.11%)	2.83	-	-	0	0	0 (0.01%)	0.09	214 (2.11%)	1.89
SUV	2 (0.02%)	0.02	2,165 (21.4%)	0.63	0	0	0	0	0	0.02	2,167 (21.4%)	0.60
Van	0	0	1,127 (11.2%)	1.53	0	0	0	0	0	0.02	1,127 (11.2%)	1.20
Taxi	-	-	-	-	0	0	-	-	-	-	0	0
Special	0	0	230 (2.28%)	2.82	0	0	-	-	-	-	230 (2.28%)	2.81
Motorcycle	0	0	-	-	-	-	-	-	-	-	0	0
Total	146 (1.44%)	0.01	9,959 (98.5%)	1.16	0	0	0	0	3 (0.03%)	0.02	10,108 (100%)	0.41

964
 965



966
 967

(d) CO

Vehicle	Gasoline		Diesel		LPG		CNG		Hybrid		Total	
	Emission	IF	Emission	IF	Emission	IF	Emission	IF	Emission	IF	Emission	IF
Sedan	178,121 (47.6%)	17.1	3,436 (0.92%)	2.98	42,886 (11.5%)	23.6	29 (0.01%)	2.91	177 (0.05%)	1.07	224,649 (60.1%)	16.6
Truck	254 (0.07%)	61.1	47,065 (12.6%)	15.2	9,088 (2.43%)	44.9	68 (0.02%)	51.4	-	-	56,475 (15.1%)	17.1
Bus	0 (0.00%)	19.3	7,633 (2.05%)	101	-	-	1542 (0.41%)	41.3	1 (0.00%)	4.64	9,176 (2.45%)	81.2
SUV	2,616 (0.70%)	19.6	13,401 (3.58%)	3.87	791 (0.21%)	38.6	0 (0.00%)	4.09	2 (0.00%)	1.15	16,808 (4.50%)	4.65
Van	131 (0.04%)	43.4	6,611 (1.77%)	8.97	8,032 (2.15%)	40.9	2 (0.00%)	6.53	0 (0.00%)	1.00	14,777 (3.95%)	15.8
Taxi	-	-	-	-	8,481 (2.27%)	14.7	-	-	-	-	8,481 (2.27%)	14.7
Special	13 (0.00%)	269	4,224 (1.13%)	51.7	1 (0.00%)	3.69	-	-	-	-	4,239 (1.13%)	51.7
Motorcycle	39,256 (10.5%)	18.2	-	-	-	-	-	-	-	-	39,256 (10.5%)	18.2
Total	220,390 (59.0%)	17.3	82,372 (22.0%)	9.57	69,281 (18.5%)	24.6	1641 (0.44%)	33.6	180 (0.05%)	1.07	373,864 (100%)	15.4

968
 969

(e) SO_x

Vehicle	Gasoline		Diesel		LPG		CNG		Hybrid		Total	
	Emission	IF	Emission	IF	Emission	IF	Emission	IF	Emission	IF	Emission	IF
Sedan	51.3 (29.8%)	0.005	6.5 (3.79%)	0.006	8.28 (4.81%)	0.005	0	0	1.14 (0.67%)	0.007	67.2 (39.1%)	0.005
Truck	0.03 (0.02%)	0.008	45.5 (26.5%)	0.015	0.97 (0.57%)	0.005	0	0	-	-	46.5 (27.1%)	0.014
Bus	0 (0.00%)	0.003	10.8 (6.26%)	0.143	-	-	0	0	0.01 (0.01%)	0.047	10.8 (6.26%)	0.095
SUV	0 (0.00%)	0.000	18.2 (10.6%)	0.005	0.00 (0.00%)	0.000	0	0	0.01 (0.01%)	0.007	18.2 (10.6%)	0.005
Van	0.02 (0.01%)	0.006	5.5 (3.20%)	0.007	0.77 (0.45%)	0.004	0	0	0 (0.00%)	0.010	6.30 (3.66%)	0.007
Taxi	-	-	-	-	7.71 (4.49%)	0.013	-	-	-	-	7.71 (4.48%)	0.013
Special	0 (0.00%)	0.003	7.3 (4.27%)	0.090	0.00 (0.00%)	0.005	-	-	-	-	7.34 (4.27%)	0.090
Motorcycle	7.94 (4.62%)	0.004	-	-	-	-	-	-	-	-	7.94 (4.62%)	0.004
Total	59.3 (34.5%)	0.006	93.8 (54.5%)	0.011	17.7 (10.3%)	0.006	0	0	1.17 (0.68%)	0.007	172 (100%)	0.007

970
 971
 972

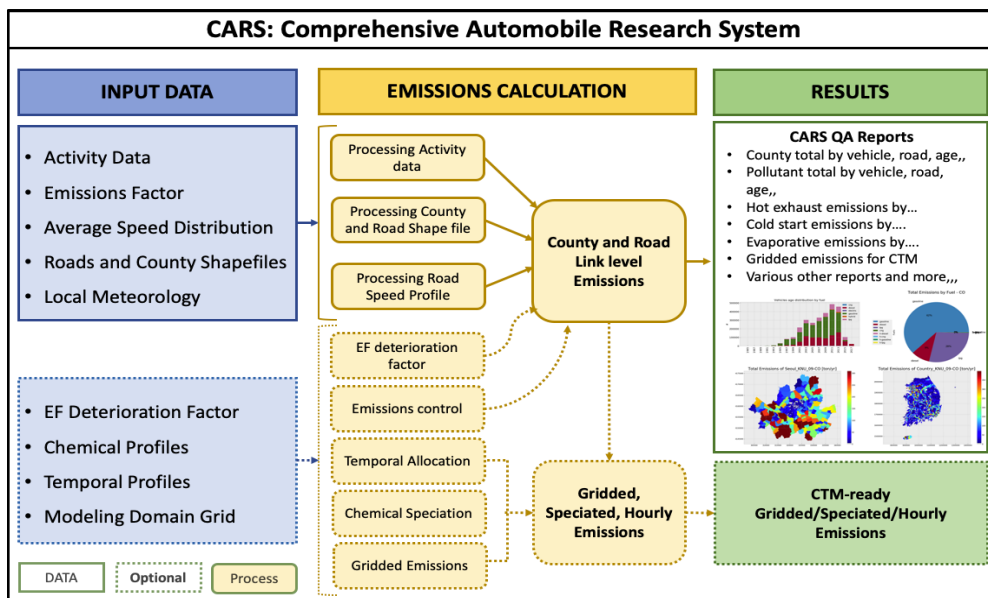
(e) NH₃

Vehicle	Gasoline		Diesel		LPG		CNG		Hybrid		Total	
	Emission	IF	Emission	IF	Emission	IF	Emission	IF	Emission	IF	Emission	IF
Sedan	12,225 (98.3%)	1.17	20 (0.16%)	0.02	0	0.00	0	0	19 (0.15%)	0.11	12,284 (98.6%)	0.91
Truck	0 (0.00%)	0.03	82 (0.66%)	0.03	0	0.00	0	0	-	-	82 (0.66%)	0.02
Bus	0 (0.00%)	0.09	15 (0.12%)	0.19	-	-	0	0	0 (0.00%)	0.51	15 (0.12%)	0.13
SUV	0 (0.00%)	0.00	0 (0.00%)	0.00	0	0.00	0	0	0 (0.00%)	0.16	0 (0.00%)	0.00
Van	0 (0.00%)	0.02	14 (0.11%)	0.02	0	0.00	0	0	0 (0.00%)	0.09	14 (0.11%)	0.01
Taxi	-	-	-	-	0	0.00	-	-	-	-	0 (0.00%)	0.00
Special	0 (0.00%)	0.01	10 (0.08%)	0.12	0	0.00	-	-	-	-	10 (0.08%)	0.12
Motorcycle	49 (0.39%)	0.02	-	-	-	-	-	-	-	-	49 (0.39%)	0.02
Total	12,293 (98.7%)	0.97	141 (1.13%)	0.02	0	0.00	0	0	19 (0.16%)	0.12	12,453 (100%)	0.51

973
 974



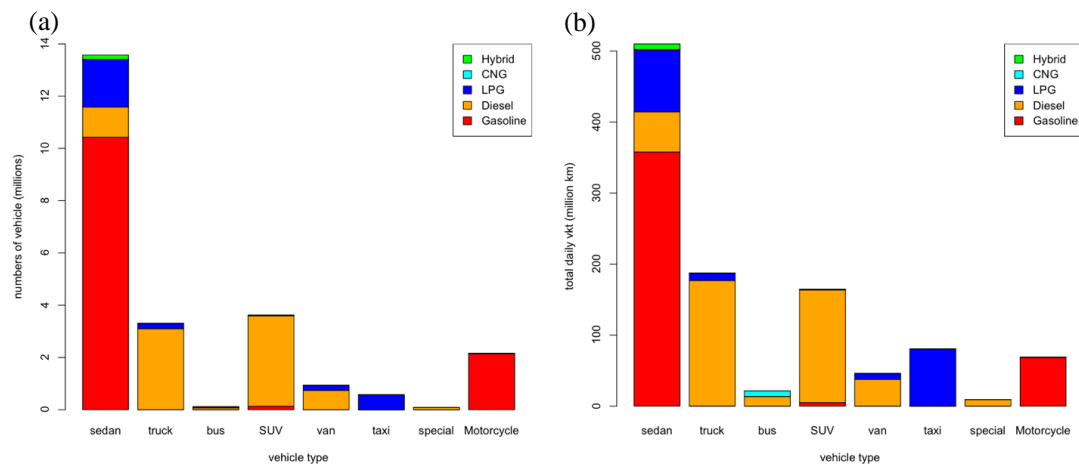
975 **Figures**



976

977 **Figure 1.** CARS schematic methodology to estimate mobile emissions.

978

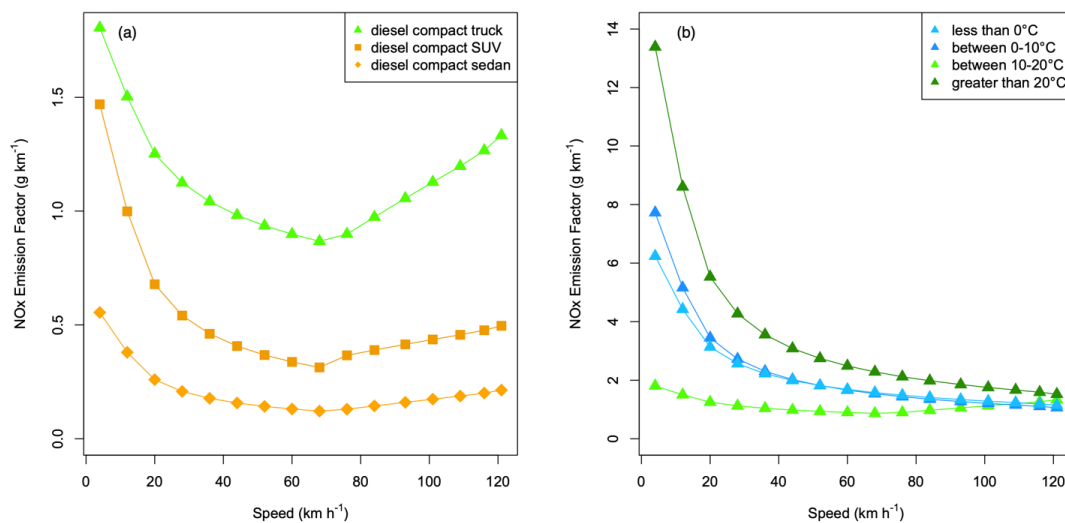


979

980 **Figure 2.** (a) The number of vehicles by vehicle and fuel types and (b) the total daily VKT by
981 vehicle and fuel types in South Korea.

982

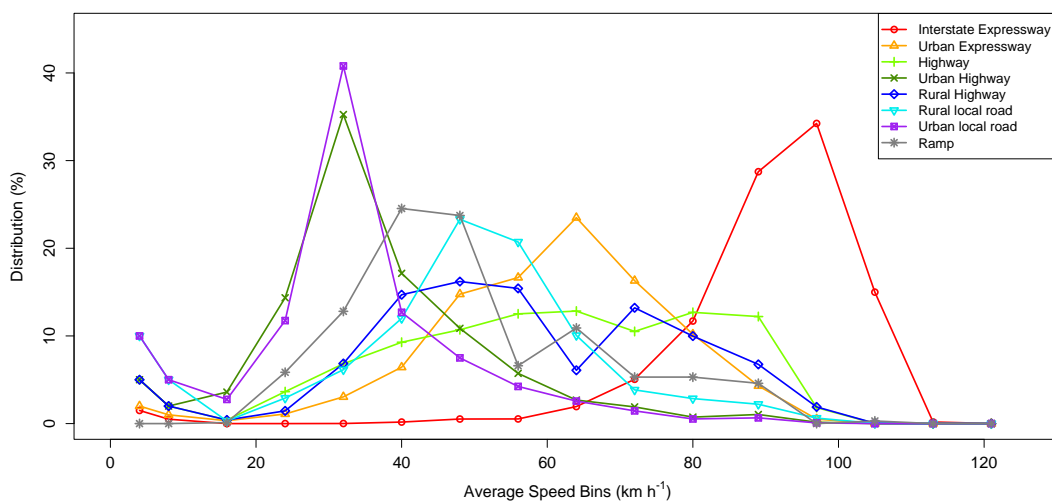
983



984

985 **Figure 3.** Variation of NO_x emission factors from diesel compact engines by vehicle speed and
986 ambient temperatures: **(a)** NO_x emission factors function to vehicle speed; **(b)** NO_x emission
987 factors of diesel compact truck function to vehicle speed and ambient temperature.

988



989
990
991
992

Figure 4. Road-specific average speed distribution (ASD) in South Korea.



993
994
995

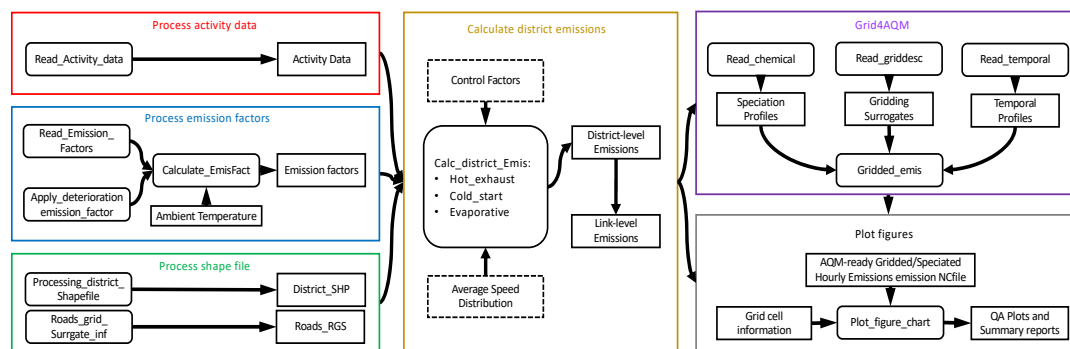
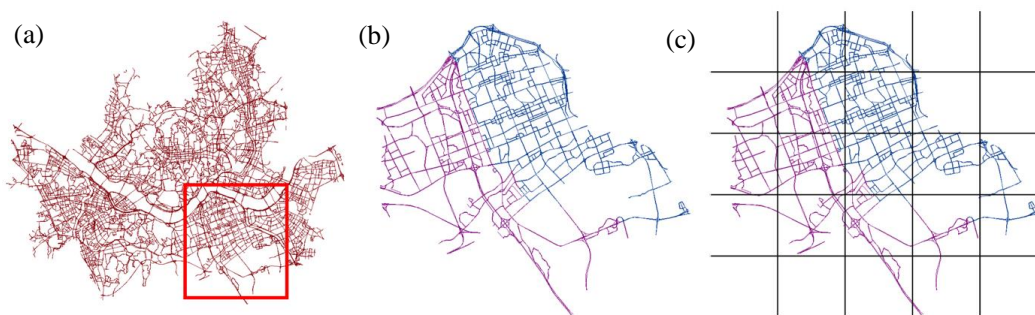
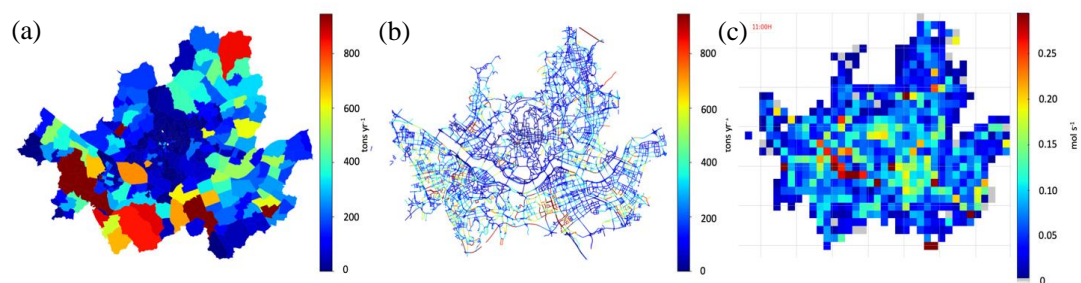


Figure 5. The schematic of modules and their functions in the CARS.



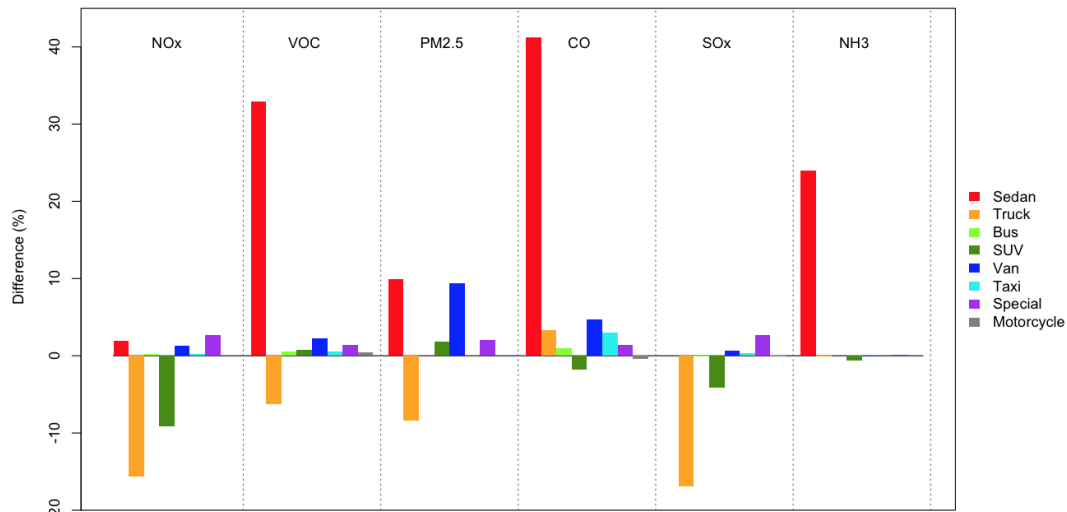
996
997 **Figure 6** (a) the road network GIS shapefile of Seoul, South Korea; (b) two districts with different
998 colors (purple and blue); (c) the modeling grid cells over road segments.
999



1000

1001 **Figure 7.** Three different formats of CO emissions from CARS, (A) District-level total emissions
1002 (t yr^{-1}) (B) Link-level total emissions (t yr^{-1}), (C) CTM-ready gridded hourly total emissions (moles
1003 s^{-1}).

1004

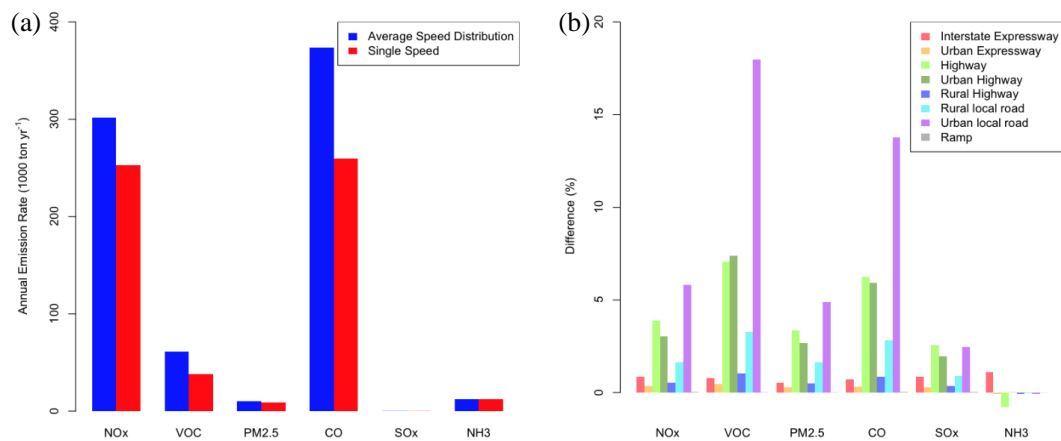


1005
1006
1007
1008

Figure 8. Comparison between CARS 2015 and CAPSS 2015 onroad mobile emissions inventories by vehicle types. The standard line is CAPSS 2015 data.



1009



1010

1011

1012

1013

Figure 9. The impacts of emissions between the ASD and single-speed approach: (a) the total emission differences by pollutant; (b) The road-specific difference (%) by pollutant.



1014 **Appendices**

1015

1016 **Appendix A:** The vehicle types classified by fuel type, vehicle body type, and engine size. The
 1017 emission factors of the diesel vehicle with the star (*) are depended on the ambient temperature
 1018 (*T*).

Vehicle Types	Fuel Types							
	Gasoline	Diesel	LPG	CNG	HYBRID_G	HYBRID_D	HYBRID_L	HYBRID_C
Sedan	Supercompact	Supercompact*	Supercompact	-	-	-	-	-
	Compact	compact*	compact	compact	compact	compact	compact	-
	Fullsize	Fullsize*	Fullsize	Fullsize	Fullsize	Fullsize	Fullsize	-
	Midsize	Midsize*	Midsize	Midsize	Midsize	Midsize	Midsize	-
Truck	Supercompact	Supercompact	Supercompact	-	-	-	-	-
	Compact	Compact*	Compact	Compact	-	-	-	-
	Fullsize	Concrete	-	Fullsize	-	-	-	-
	Midsize	Fullsize	Midsize	Midsize	-	-	-	-
	-	Midsize	-	-	-	-	-	-
	-	Dump	-	-	-	-	-	-
Bus	Urban	Urban	Urban	Urban	-	Urban	-	-
	-	Rural	-	Rural	-	Rural	-	Rural
SUV	Compact	Compact*	Compact	-	-	-	-	-
	Midsize	Midsize*	Midsize	Midsize	Midsize	-	-	-
Van	supercompact	supercompact	supercompact	-	-	-	-	-
	Compact	Compact	Compact	Compact	-	-	-	-
	-	-	Fullsize	Fullsize	Fullsize	Fullsize	Fullsize	Fullsize
Taxi	Midsize	Midsize	Midsize	Midsize	Midsize	Midsize	Midsize	Midsize
	-	-	Compact	-	-	-	-	-
Special	-	-	Fullsize	-	-	-	-	-
	-	-	Midsize	-	-	-	-	-
	Wrecking	Tow	-	Wrecking	-	-	-	-
Motorcycle	Others	Wrecking	Wrecking	Wrecking	-	-	-	-
	Others	Others	Others	-	-	-	-	-
	Compact	-	-	-	-	-	-	-
Motorcycle	Midsize	-	-	-	-	-	-	-
	Fullsize	-	-	-	-	-	-	-

- 1019 - no existence
- 1020 * ambient temperature-dependent diesel vehicle
- 1021 LPG: Liquefied Petroleum Gas
- 1022 CNG: Connecticut Natural Gas
- 1023 Hybrid_G: hybrid vehicle with gasoline
- 1024 Hybrid_D: hybrid vehicle with diesel
- 1025 Hybrid_L: hybrid vehicle with LPG
- 1026 Hybrid_C: hybrid vehicle with CNG
- 1027
- 1028



1029 **Appendix B**, The summary of activity data (number of vehicles and daily total VKTs) in South
 1030 Korea by vehicle type with engine size.

Vehicle Types	Engine sizes	Fuel Types									
		Gasoline		Diesel		LPG		CNG		Hybrid	
		Numbers	Daily VKT	Numbers	Daily VKT	Numbers	Daily VKT	Numbers	Daily VKT	Numbers	Daily VKT
Sedan	Supercompact	1,792,471	50,197,345	46	1,761	83,226	4,000,067	6	237	-	-
	Compact	1,372,317	39,543,668	51,324	2,570,086	8,040	257,060	276	12,115	3,802	137,360
	Fullsize	2,403,327	100,632,702	428,831	20,928,552	292,850	15,910,588	5,296	323,852	21,533	1,086,509
	Midsize	4,858,533	167,454,032	672,960	33,126,318	1,431,970	66,640,378	4,310	625,717	140,527	6,717,856
Truck	Supercompact	850	9,595	816	354	111,051	6,550,476	-	-	-	-
	Compact	3,185	143,510	2,655,089	133,480,216	87,650	3,567,109	42	2,694	-	-
	Fullsize	3	422	180,991	25,774,819	-	-	72	4,676	-	-
	Midsize	98	7,430	258,509	17,477,685	1,434	47,870	14	483	-	-
	Dump	-	-	-	-	-	-	-	-	-	-
	Special	20	970	-	-	2,292	99,124	1,194	60,886	-	-
Bus	Urban	1	126	40,448	7,282,593	1	652	6,543	1,466,854	2	282
	Rural	-	-	34,997	6,334,278	-	-	30,792	6,460,001	216	50,873
SUV	Compact	42,348	1,395,153	2,341,397	105,962,626	6,946	275,728	13	551	-	-
	Midsize	91,002	3,520,552	1,120,128	5,277,861	13,567	595,426	15	706	1,719	88,683
Van	supercompact	88	1,645	-	-	44,947	2,058,014	-	-	-	-
	Compact	2,937	87,507	685,317	34,781,937	151,654	6,135,138	7	255	-	-
	Fullsize	-	-	19,452	1,318,221	1	14	97	7,598	3	136
	Midsize	2	1,303,795	31,790	1,433,407	15	416	160	15,216	2	85
Taxi	Special	-	-	-	-	-	-	-	-	-	-
	Compact	-	-	-	-	8,380	576,378	-	-	-	-
	Fullsize	-	-	-	-	92,861	10,827,756	-	-	-	-
Special	Midsize	-	-	-	-	474,455	69,087,721	-	-	-	-
	Tow	-	-	40,807	7,447,773	-	-	-	-	-	-
	Wrecking	2	138	12,568	813,746	128	6,607	3	94	-	-
Motorcycle	Others	47	553	28,275	989,988	180	9,966	-	-	-	-
	Compact	184,822	3,507,948	-	-	-	-	-	-	-	-
	Fullsize	65,964	3,493,728	-	-	-	-	-	-	-	-
Motorcycle	Midsize	1,910,988	61,676,824	-	-	-	-	-	-	-	-

- 1031 - no existence
- 1032 LPG: Liquefied Petroleum Gas
- 1033 CNG: Connecticut Natural Gas
- 1034 Hybrid: all hybrid vehicles, electric power mixed with fossil fuel (gasoline, diesel, LPG, or CNG)
- 1035
- 1036
- 1037



1038

1039 **Appendix C**, Eight road types with assigned average vehicle operating speed and VKT fractions.

Road types	Description	Average Speed (km h ⁻¹)	Road VKT fraction
101	Interstate Expressway	90	41%
102	Urban Expressway	60	5%
103	Highway	58	18%
104	Urban Highway	36	12%
105	Rural Highway	55	3%
106	Rural Local Road	45	4%
107	Urban Local Road	32	17%
108	Ramp	50	0.4%

1040

1041

1042 **Appendix D**, The daily average VKT (km d⁻¹) per vehicle by vehicle and fuel types.

Vehicle types	Fuel Types					
	Gasoline	Diesel	LPG	CNG	Hybrid	Average
Sedan	34	49	48	97	48	38
Truck	39	57	51	52	-	57
Bus	126	180	-	212	237	191
SUV	37	46	42	45	52	46
VAN	29	51	42	87	44	49
Taxi	-	-	140	-	-	140
Special	14	113	54	31	-	113
Motorecycle	32	-	-	-	-	32

1043

1044



1045 **Appendix E**, Average speed distribution (ASD) for each road type: The table columns are
 1046 different road types, and the table rows are average speed of each speed bin.

Speed (km/d)	Road Types							
	101	102	103	104	105	106	107	108
4	1.50%	2.00%	5.00%	5.00%	5.00%	10.00%	10.00%	0.00%
8	0.50%	1.00%	2.00%	2.00%	2.00%	5.00%	5.00%	0.00%
16	0.00%	0.33%	0.40%	3.59%	0.41%	0.30%	2.76%	0.11%
24	0.00%	1.09%	3.64%	14.35%	1.45%	2.91%	11.75%	5.85%
32	0.01%	3.04%	6.82%	35.25%	6.85%	6.15%	40.80%	12.80%
40	0.17%	6.43%	9.28%	17.14%	14.70%	12.00%	12.69%	24.53%
48	0.52%	14.76%	10.70%	10.86%	16.20%	23.30%	7.49%	23.74%
56	0.53%	16.66%	12.52%	5.72%	15.42%	20.72%	4.24%	6.60%
64	1.94%	23.49%	12.83%	2.68%	6.08%	10.06%	2.56%	10.90%
72	5.05%	16.30%	10.51%	1.90%	13.21%	3.84%	1.45%	5.30%
80	11.70%	10.19%	12.69%	0.74%	9.98%	2.85%	0.53%	5.30%
89	28.73%	4.30%	12.21%	1.04%	6.75%	2.21%	0.65%	4.59%
97	34.24%	0.51%	1.82%	0.15%	1.90%	0.62%	0.08%	0.00%
105	14.99%	0.00%	0.02%	0.00%	0.04%	0.03%	0.00%	0.30%
113	0.18%	0.00%	0.00%	0.00%	0.00%	0.00%	0.00%	0.00%
121	0.01%	0.00%	0.00%	0.00%	0.00%	0.00%	0.00%	0.00%

1047 **Appendix F**: A single-speed for each road type

Speed (km/d)	Road Types							
	101	102	103	104	105	106	107	108
4	0%	0%	0%	0%	0%	0%	0%	0%
8	0%	0%	0%	0%	0%	0%	0%	0%
16	0%	0%	0%	0%	0%	0%	0%	0%
24	0%	0%	0%	0%	0%	0%	0%	0%
32	0%	0%	0%	0%	0%	0%	100%	0%
40	0%	0%	0%	100%	0%	0%	0%	0%
48	0%	0%	0%	0%	0%	100%	0%	100%
56	0%	0%	100%	0%	100%	0%	0%	0%
64	0%	100%	0%	0%	0%	0%	0%	0%
72	0%	0%	0%	0%	0%	0%	0%	0%
80	0%	0%	0%	0%	0%	0%	0%	0%
89	100%	0%	0%	0%	0%	0%	0%	0%
97	0%	0%	0%	0%	0%	0%	0%	0%
105	0%	0%	0%	0%	0%	0%	0%	0%
113	0%	0%	0%	0%	0%	0%	0%	0%
121	0%	0%	0%	0%	0%	0%	0%	0%

1048